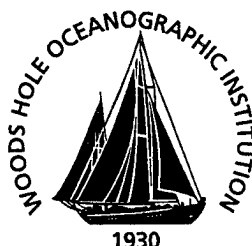


# Woods Hole Oceanographic Institution



---

## Evaluation of NSCAT Scatterometer Winds Using Equatorial Pacific Buoy Observations

*by*

Michael J. Caruso  
Suzanne Dickinson  
Kathryn A. Kelly  
Mick Spillane  
Linda J. Mangum  
Michael J. McPhaden  
Linda D. Stratton

July 1999

**Technical Report**

**19991004 049**

Funding was provided by the National Aeronautics and Space Administration  
under Contract No. 957652.

Approved for public release; distribution unlimited.

WHOI-99-10

# **Evaluation of NSCAT Scatterometer Winds Using Equatorial Pacific Buoy Observations**

by

Michael J. Caruso  
Suzanne Dickinson  
Kathryn A. Kelly  
Mick Spillane  
Linda J. Mangum  
Michael J. McPhaden  
Linda D. Stratton

Woods Hole Oceanographic Institution  
Woods Hole, Massachusetts 02543

July 1999


## **Technical Report**

Funding was provided by the National Aeronautics and Space Administration  
under Contract No. 957652.

Reproduction in whole or in part is permitted for any purpose of the United States  
Government. This report should be cited as Woods Hole Oceanog. Inst. Tech. Rept.,  
WHOI-99-10.

Approved for public release; distribution unlimited.

Approved for Distribution:

  
\_\_\_\_\_  
Terrence M. Joyce, Chair

Department of Physical Oceanography

# Evaluation of NSCAT Scatterometer Winds Using Equatorial Pacific Buoy Observations

Michael J. Caruso

Woods Hole Oceanographic Institution

Woods Hole, MA

Suzanne Dickinson

Kathryn A. Kelly

Mick Spillane

Applied Physics Laboratory

University of Washington

Seattle, WA

Linda Mangum

Michael McPhaden

Linda Stratton

Pacific Marine Environmental Laboratory

Seattle, WA

July 21, 1999

### Abstract

As part of the calibration/validation effort for NASA's Scatterometer (NSCAT) we compare the satellite data to winds measured at the sea surface with an array of buoys moored in the equatorial Pacific Ocean. The NSCAT data record runs from September, 1996 through the end of June, 1997. The raw NSCAT data, radar backscatter, is converted to wind vectors at 10 meters above the surface assuming a neutrally stratified atmosphere, using the NSCAT-1 and NSCAT-2 model functions. The surface winds were measured directly by the TAO (Tropical Atmosphere Ocean) buoy array which spans the width of the equatorial Pacific within about  $8^\circ$  of the equator. The buoy program and data archive are maintained by the Pacific Marine Environmental Laboratory, at the National Oceanic and Atmospheric Administration, in collaboration with institutions in Japan, France and Taiwan. We also use data from two buoys maintained by the Woods Hole Oceanographic Institution located along  $125^\circ\text{W}$ . Since the buoy winds are measured at various heights above the surface, they are adjusted for both height and atmospheric surface layer stratification before comparisons are made to the NSCAT data. Co-location requirements include measurements within 100 km and 60 minutes of each other. There was a total of 5580 comparisons for the NSCAT-1 model function and 6364 comparisons for the NSCAT-2 model function. The NSCAT wind speeds, using the NSCAT-1 model function, are lower than the buoy wind speeds by about  $0.54 \text{ ms}^{-1}$  and have a  $9.8^\circ$  directional bias. The NSCAT-2 winds speeds were lower than the TAO buoy winds by only  $0.08 \text{ ms}^{-1}$ , but still have the same  $9.8^\circ$  directional bias. The wind retrieval algorithm selects the vector closest to the buoy approximately 88% of the time. However, in the relatively low wind speed regime of the TAO array, approximately 4% of the wind vectors are more than  $120^\circ$  from the buoy wind.

# Contents

<b>1</b>	<b>Introduction</b>	<b>6</b>
<b>2</b>	<b>Data Sets</b>	<b>7</b>
2.1	NASA Scatterometer . . . . .	7
2.2	TAO array . . . . .	7
2.3	WHOI buoys . . . . .	12
<b>3</b>	<b>Data preparation</b>	<b>14</b>
3.1	Conversion to 10 m in Neutral Stratification . . . . .	14
3.2	Co-location . . . . .	14
3.2.1	File format . . . . .	14
<b>4</b>	<b>Wind Comparisons</b>	<b>19</b>
4.1	Instrument accuracies . . . . .	20
4.2	TAO wind comparisons . . . . .	21
4.3	Interpretation of the speed bias . . . . .	28
4.4	WHOI wind comparisons . . . . .	31
4.4.1	Combined IMET and VAWR winds . . . . .	31
4.4.2	IMET winds . . . . .	34
4.4.3	VAWR winds . . . . .	37
4.4.4	TAO/WHOI . . . . .	40
4.5	Wind speed distributions . . . . .	43
4.6	Wind direction distributions . . . . .	45
4.7	Vector correlations . . . . .	47
4.8	Directional Ambiguity . . . . .	49
4.9	Surface currents . . . . .	56
4.10	Rain . . . . .	56
<b>5</b>	<b>Summary</b>	<b>57</b>
<b>6</b>	<b>References</b>	<b>59</b>

## LIST OF FIGURES

---

### List of Figures

1	TAO buoy configuration . . . . .	9
2	Buoy locations. . . . .	11
3	Co-locations for each TAO buoy. . . . .	11
4	WHOI discus buoy schematic. . . . .	13
5	Scatterplots of wind speeds and directions derived from 25 km high resolution winds with TAO 10 m buoy winds. . . . .	24
6	NSCAT-1 25 km high resolution wind speeds and directions binned against TAO 10 m buoy winds. . . . .	25
7	NSCAT-1 50 km wind speeds and directions binned against TAO 10 m buoy winds. . . . .	26
8	NSCAT-2 25 km wind speeds and directions binned against TAO 10 m buoy winds. . . . .	27
9	Biases of scatterometer winds relative to buoy measurements . . . . .	29
10	Zonal and meridional component scatterplots of TAO buoy and NSCAT winds. . . . .	30
11	Scatterplots of wind speeds and directions derived from 25 km high resolution winds with WHOI 10 m buoy winds. . . . .	33
12	Scatterplots of wind speeds and directions derived from 25 km high resolution winds with WHOI IMET 10 m buoy winds. . . . .	36
13	Scatterplots of wind speeds and directions derived from 25 km high resolution winds with WHOI VAWR 10 m buoy winds. . . . .	39
14	Scatterplots of wind speeds and directions derived from 25 km high resolution NSCAT data (top) and 50 km standard product (bottom) with TAO 51017 and 51307 10 m buoy winds. . . . .	42
15	Wind speed distributions of TAO and NSCAT 10 m buoy winds. . . . .	43
16	Wind speed distributions of WHOI and NSCAT 10 m buoy winds. . . . .	44
17	Wind direction distributions of TAO and NSCAT 10 m buoy winds. . . . .	45
18	Wind direction distributions of NSCAT and WHOI IMET 10 m and VAWR 10 m buoy directions. . . . .	46
19	Vector correlation coefficient for each TAO buoy. . . . .	48
20	Percentage flipped vectors as a function of TAO buoy wind speed. . . . .	52
21	Percentage of flipped vectors from NSCAT-1 as a function of TAO buoy wind direction. . . . .	53
22	NSCAT vector flipped relative to TAO. . . . .	54
23	Scatterplots of wind speeds and directions for NSCAT and TAO when direction differences are less than 60° or 90°. . . . .	55

## *LIST OF FIGURES*

---

24	Wind speed difference dependence on the angle between wind and surface current. . . . .	56
----	---	----

## LIST OF TABLES

---

### List of Tables

1	TAO buoy locations. . . . .	10
2	NSCAT co-located data file layout. . . . .	15
3	NSCAT co-located data parameters. . . . .	16
4	NSCAT co-located $\sigma_0$ parameters. . . . .	17
5	Buoy Co-located data parameters. . . . .	18
6	Instrument accuracies . . . . .	20
7	Comparison of NSCAT wind speeds and directions with TAO buoy 10 m winds. . . . .	23
8	Comparison of NSCAT wind speeds and directions with WHOI buoy 10 m winds. . . . .	32
9	Comparison of NSCAT wind speeds and directions with WHOI buoy IMET 10 m winds. . . . .	35
10	Comparison of NSCAT wind speeds and directions with WHOI buoy VAWR 10 m winds. . . . .	38
11	Comparison of NSCAT wind speeds and directions with TAO buoys 51017 and 51307 10 m winds. . . . .	41
12	Ambiguity closest to TAO buoy direction . . . . .	50
13	Ambiguity closest to WHOI buoy IMET direction . . . . .	51
14	Ambiguity closest to WHOI buoy VAWR direction . . . . .	51



# 1 Introduction

The calibration/validation effort for the NASA scatterometer (NSCAT) is intended to determine and correct systematic errors, if any, in the wind retrieval algorithm. One aspect of this effort is to compare the remotely measured satellite winds with directly measured sea surface wind vectors from buoys. In this report, we analyze the NSCAT wind retrievals in the climatically sensitive region of the tropical Pacific Ocean. Data from the Tropical Atmosphere Ocean (TAO) buoy array maintained by the Pacific Marine Environmental Lab (PMEL) of NOAA and from two buoys maintained by the Woods Hole Oceanographic Institution are used in this study.

Comparison studies for scatterometers have shown good agreement, for the most part, between the satellite data and buoy data in the past, (Graber *et al.*, 1996 and Rufenach, 1998). However, they also show that there are significant differences between the various algorithms used to derive the winds; in general, the scatterometer winds are biased low relative to the buoy winds and have direction problems at low wind speeds. Use of the TAO data provides an excellent opportunity to study the scatterometer wind estimates in a region where winds are relatively low. In addition, the mean winds in the equatorial Pacific ocean are predominately easterly. This provides a consistent wind at speeds at which the scatterometer has directional problems.

The processing of the NSCAT retrieved winds has changed several times during the calibration and validation of the instrument. The original wind fields were processed using the SASS-II geophysical model function (GMF) developed for the Seasat A Satellite Scatterometer (Wentz *et al.*, 1984). The SASS-II model function was only used for pre-launch testing and the initial analysis of NSCAT data. After the initial calibration period, SASS-II was replaced by the first NSCAT specific model function NSCAT-1, developed by Wentz and Smith (1999) using comparisons with National Centers for Environmental Prediction (NCEP) winds. The GMF was refined again after calibration with ship and buoy winds to produce the final NSCAT model function (NSCAT-2) (Freilich *et al.*, 1999), which slightly increased the wind speeds, but made no significant changes to direction. This report describes the differences between the wind fields derived from the NSCAT-1 and NSCAT-2 model functions when compared with buoy winds in the equatorial Pacific. The NSCAT-1 winds were analyzed for both 25 km and 50 km winds. However, the 50 km NSCAT-2 winds were not analyzed due to the similarities between the 25 km and 50 km NSCAT-1 winds.

This work is in parallel with other NSCAT validation studies. Graber *et al.* (1999 in progress) is performing a global validation using buoys from the National Data Buoy Center (NDBC), TAO, the Japan Meteorological Agency (JMA) and Europe (Météo-France and United Kingdom Meteorological Office). Freilich and Dunbar (1999) have also examined the accuracy of NSCAT winds compared with NDBC buoys.

---

## 2 Data Sets

### 2.1 NASA Scatterometer

The NSCAT instrument was launched aboard the Japanese Advanced Earth Observing Satellite (ADEOS-I) on August 16, 1996. The scatterometer was turned on September 9th and the Wind Observation Mode (WOM) began September 15th. Unfortunately, the scatterometer was lost on June 30, 1997 due to a power failure aboard ADEOS-I.

The ADEOS-I satellite was in a polar orbit, circling the earth approximately 14 times daily. The NASA scatterometer scans two 600 km wide swaths, one to each side of the satellite subtrack. The scatterometer uses a Ku-band (14 GHz) microwave radar to provide surface wind vectors over 90% of the ice free ocean every two days in all weather conditions. The scatterometer does not measure wind velocity directly; rather it is an active microwave instrument that measures the signal backscattered from the ocean surface. A model function uses the relationship between the frequency of the radar, the incidence angle and returned power to empirically determine the wind velocity.

The current model function (NSCAT-2), was developed by Freilich *et al.* (1999) using the wind analyses from the European Centre for Medium-Range Weather Forecasting (ECMWF) and those from the U.S. National Centers for Environmental Prediction (NCEP) and also by Wentz and Smith (1999) who used co-located Special Sensor Microwave/Imager (SSM/I) wind speed data as well as histograms of the ECMWF surface wind speeds. The model function produces up to four wind vector solutions, commonly called ambiguities. A median filter algorithm described in the NSCAT User's Manual (JPL, 1998) was used to select the correct ambiguity.

After the launch of NSCAT and the initial calibration of the 50 km data product (JPL, 1998), a high resolution (25 km) wind product was developed (Dunbar, 1997). The (25 km) wind product contains 48 wind vector cells per scan line instead of the 24 provided by the standard data product. The wind retrieval process is the same for both the standard product and the high resolution product.

### 2.2 TAO array

The Tropical Atmosphere Ocean (TAO) array consists of nearly 70 Autonomous Temperature Line Acquisition System (ATLAS) and current meter moorings (figure 1). The TAO array was developed by PMEL as a economical way to provide real-time observations of critical surface and subsurface measurements. Implementation of the array (McPhaden, 1995) was completed in 1994 with the assistance of international partners which presently include Japan, France and Taiwan.

The TAO array covers the tropical Pacific from approximately 8°S to 8°N, 95°W to 137°E. The locations of the TAO buoys used in this comparison are listed in table 1 and shown geographically in figure 2. Standard measurements on all TAO buoys include surface winds, relative humidity, air temperature, sea surface and subsurface temperatures. The temperature and relative humidity are sampled every 10 minutes starting at 10 minutes past the hour and averaged at the top of the hour. Winds are sampled at 2Hz for 6 minutes centered on the top of the hour and then vector averaged (Mangum *et al.*, 1994).

Although hourly sampled data are recorded on board each buoy, satellite transmissions are limited to two 4-hour periods per day in order to conserve battery power. As a result, "real-time" data typically consists of 3 or 4 hourly reports per day (generally not consecutive) together with daily averages computed from the full set of internally recorded hourly observations. During the NSCAT mission, four buoys also contained rain gauges with a full set of hourly rain data telemetered daily.

The hourly data record is retrieved when the buoys are serviced during twice yearly cruises. The retrieved data were processed and quality controlled at PMEL, subjected to additional quality control at APL, becoming available 2 - 3 weeks after the cruise ended. Cruises are staggered in time throughout the year with only a subset of array longitudes visited each time. Additional retrievals were made on the servicing cruises during the NSCAT mission to expedite the wind comparisons. The number of valid co-locations for each buoy is shown in figure 3.

## 2.2 TAO array

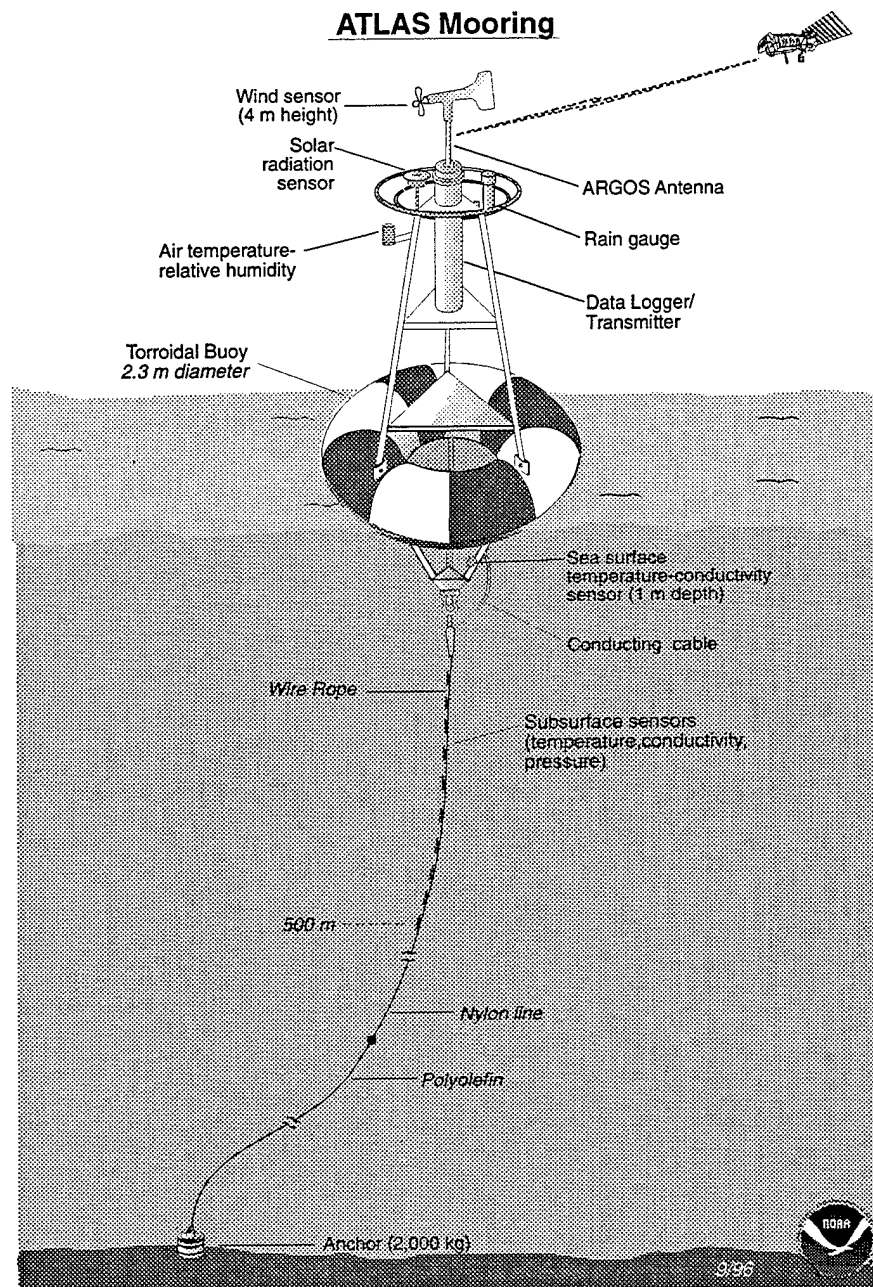


Figure 1: A typical TAO buoy configuration. The atmospheric sensors are located at 3 m height and the wind sensor is located at 4 m height. Only 4 of the buoys were equipped with rain gauges during the NSCAT mission.

Station Id	Latitude	Longitude	Station Id	Latitude	Longitude
32303	5.08° N	94.94° W	51305	1.96° N	170.00° W
32304	5.01° S	95.08° W	51306	2.15° S	170.02° W
32305	8.02° S	95.08° W	51307	8.04° N	125.01° W
32315	4.99° N	109.92° W	51308	7.99° S	125.00° W
32316	2.04° N	110.11° W	51309	8.03° N	170.01° W
32317	2.00° S	109.99° W	51310	8.00° S	170.06° W
32318	4.97° S	109.97° W	51311	0.03° N	139.92° W
32319	8.06° S	109.92° W	52001	2.00° N	164.93° E
32321	0.03° S	94.99° W	52002	1.94° S	164.35° E
32322	1.99° S	95.00° W	52003	5.05° N	165.00° E
32323	0.00° N	109.92° W	52004	5.00° S	165.21° E
43001	8.05° N	110.14° W	52006	8.01° N	165.02° E
43301	8.05° N	94.96° W	52007	8.03° S	164.84° E
51006	9.01° N	140.27° W	52008	5.00° N	156.07° E
51007	4.89° N	139.84° W	52010	5.00° S	156.00° E
51008	1.97° N	139.98° W	52011	2.03° N	156.02° E
51009	2.01° S	139.95° W	52012	2.00° S	155.99° E
51010	0.03° S	170.03° W	52301	2.00° N	146.99° E
51011	0.02° S	124.34° W	52302	4.96° N	147.04° E
51014	5.01° S	139.90° W	52307	2.44° N	137.41° E
51015	5.13° N	124.86° W	52309	4.99° N	179.96° W
51016	1.97° N	125.08° W	52310	2.01° N	179.79° W
51017	1.99° S	124.96° W	52311	0.01° N	179.89° W
51018	5.02° S	124.93° W	52312	1.99° S	179.87° W
51019	5.00° S	154.99° W	52313	5.03° S	179.90° W
51020	4.99° N	154.92° W	52314	5.00° N	136.97° E
51021	2.05° N	154.93° W	52315	8.01° N	179.88° W
51022	1.98° S	155.01° W	52316	7.97° S	179.84° W
51023	0.00° N	154.98° W	52317	0.01° N	156.16° E
51301	7.97° N	154.99° W	52318	0.00° N	146.99° E
51302	8.28° S	154.96° W	52319	8.00° N	156.00° E
51303	4.97° N	169.92° W	52320	6.76° N	137.68° E
51304	4.99° S	170.00° W	52321	0.00° N	164.99° E

Table 1: The TAO buoy locations as reported at the beginning of the NSCAT mission. The reported buoy location is used for the co-location process.

# 2.2 TAO array

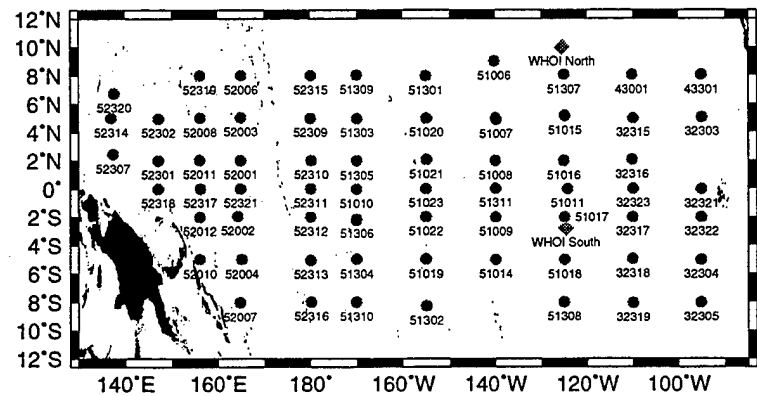


Figure 2: Locations of the 66 TAO buoys (●) and the two WHOI buoys (◇) used in this study. The numbers are the WMO buoy identification numbers. The two WHOI buoys are located along 125°W.

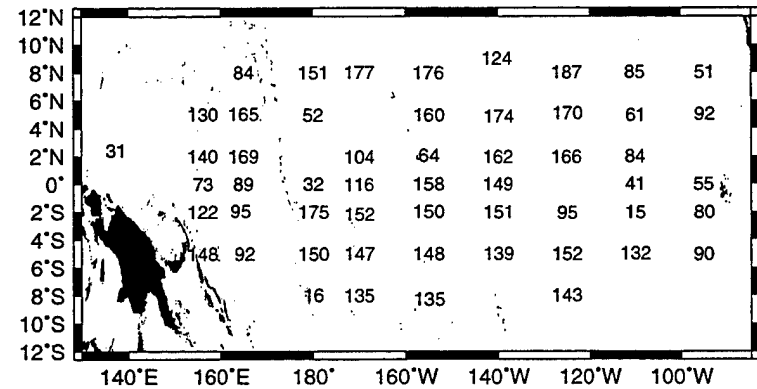
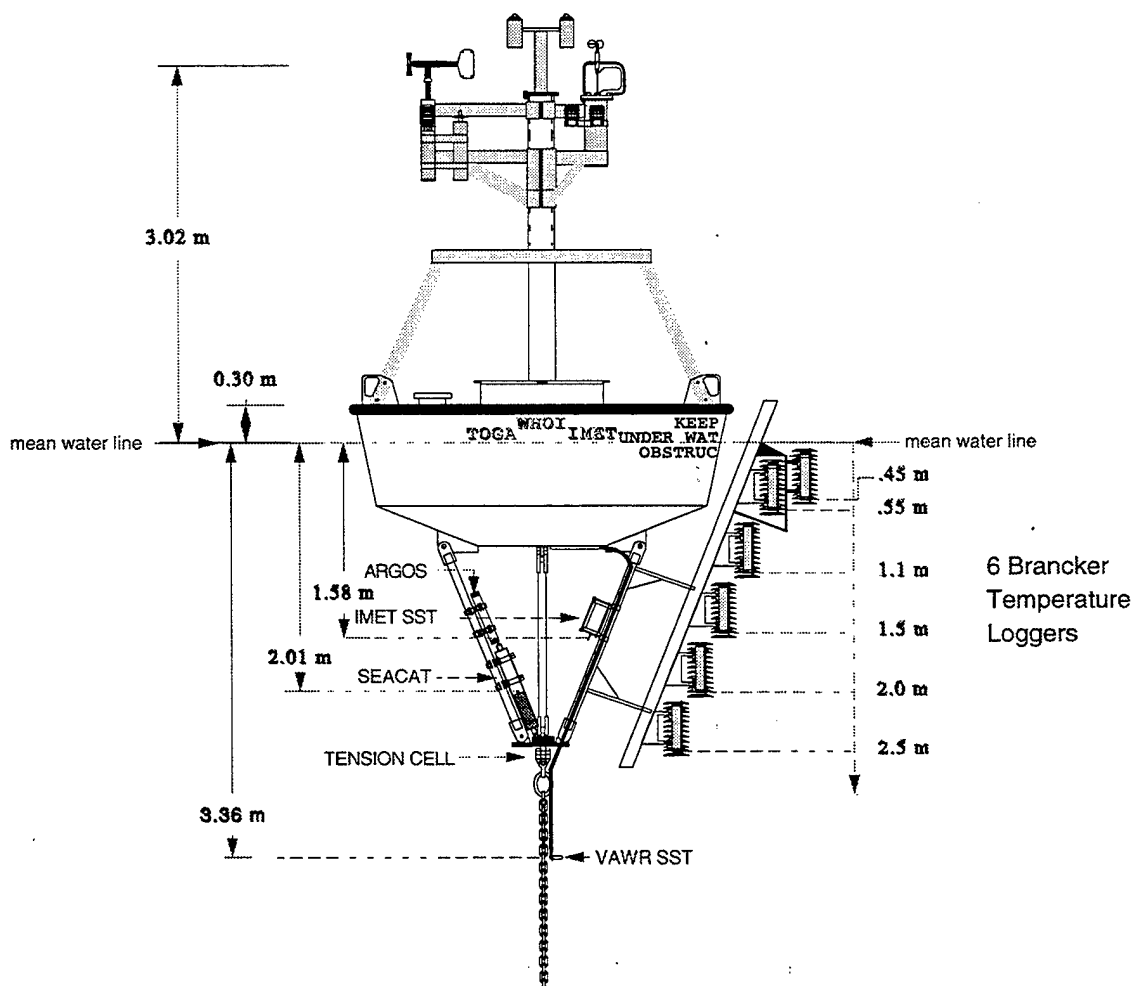


Figure 3: Number of valid co-locations obtained at each TAO buoy. There are 87 co-locations for WHOI North and 81 co-locations for WHOI South.

### 2.3 WHOI buoys

Two Woods Hole Oceanographic Institution (WHOI) surface moorings were deployed in April 1997 as part of the Pan-American Climate Study (PACS). These buoys were set at 3°S and 10°N along 125°W. Each buoy has two complete sets of meteorological instruments. Each set includes the Improved METeorology (IMET) package (Hosom *et al.*, 1995) and a Vector Averaging Wind Recorder (VAWR) package. The anemometers are mounted at 3.3 m, the relative humidity sensor is mounted at 2.5 m and the air temperature sensor is mounted 2.4 m above the water line. The sea surface temperature sensor is located 0.45 m below the water line. The schematic for a typical WHOI discus buoy is shown in figure 4.

## WHOI DISCUS BUOY



W.Ostrom  
1/28/94  
W.H.O.I.- U.O.P.G.

Figure 4: The schematic for a typical WHOI discus buoy. The anemometer heights for the PACS buoys were 3.3 m above the water line. The air temperature and relative humidity sensors are located at 2.4 m and 2.5 m respectively



## 3 Data preparation

### 3.1 Conversion to 10 m in Neutral Stratification

The TAO buoy anemometers are all 4.0 m (figure 1) above the surface of the water and the WHOI buoys are at 3.3 m (figure 4). The NSCAT model function, however, produces winds estimated at 10 m above the surface, in equivalent neutral stratification. Using the complementary data collected at the buoys, air and sea temperature and relative humidity, the buoy winds are normalized to 10 m in neutral stratification before doing the comparisons. The bulk formulation of Liu *et al.* (1979), more commonly called the LKB formulation is used. An iterated solution is computed on the roughness lengths and the scaling parameters of the wind, temperature and humidity profiles in the atmospheric surface layer. When the necessary complementary data are not available, estimates are used. A missing humidity datum is assumed to be 75% and the atmospheric pressure is assumed to be 1013.25 mb for the TAO buoys and missing WHOI measurements (Liu and Tang, 1996). All other parameters are required for a 10 m estimate. A typical adjustment to the measured wind speed was  $0.6 \text{ ms}^{-1}$ .

### 3.2 Co-location

The co-location process is performed for each NSCAT science data product (NSP). The 50 km data product includes the ocean wind vectors (Level 2.0) and the grouped  $\sigma_o$ 's (Level 1.7) in separate files. The High-Resolution Merged Geophysical Data Product (HR-MGDR) or Global 25 km GDR (Level 2.5) combines the Earth-located radar backscatter and wind measurements. The hourly buoy data are split into weekly files coincident with each NSP to reduce the processing time. Each buoy measurement is checked against each swath. If a match is found where the data are within 1 hour and 100 km of each other, the data pair are kept and sorted by distance between buoy and wind vector cell. The four closest co-locations in space are retained with the buoy observations at the hour previous and following the scatterometer measurement. Buoy measurements for the time before (n) and after (n+1) the WVC measurement are kept to analyze any changes that occur in the buoy measurements.

To maximize the potential number of co-locations available for comparison, all pairs are kept at this stage. The flagging of pairs that contain missing or bad buoy or NSCAT data records is left to the analysis stage.

#### 3.2.1 File format

The co-location format file is in ASCII format and contains 331 columns of data. Table 2 shows the layout of the file. The file contains the four closest WVCs for each co-location and

### 3.2 Co-location

---

the buoy record prior to and following the NSCAT overpass. Table 3 lists the scatterometer wind parameters; table 4 contains the  $\sigma_o$  parameters and table 5 lists the buoy parameters.

Group	Columns	Description
1	1	WMO identification number
2	73	Closest NSCAT WVC
3	73	Second closest NSCAT WVC
4	73	Third closest NSCAT WVC
5	73	Fourth closest NSCAT WVC
6	28	Buoy record at time prior to NSCAT time
7	28	Buoy record at time following NSCAT time
<b>Total</b>	349	

Table 2: NSCAT co-located data layout. Each record has the buoy identification number in the first column. The four closest WVCs follow sorted by distance to the buoy. The last two groups contain the buoy data prior to and following the NSCAT overpass.

Column	Offset	Name	Description
<i>Identifier</i>			
1	1	Buoy ID	WMO identifier e.g. 51309
<i>NSCAT</i>			
2	1	nsorb	Orbit number; e.g. 00414
3	2	nsrec	Record number along swath; 1 – 1624
4	3	nsyear	Year; e.g. 1997
5	4	nsmon	Month of year; 1–12
6	5	nsday	Day of month; 1–31
7	6	nshour	Hour of day; 0 – 23
8	7	nsmin	Minute of hour; 0 – 59
9	8	nssec	Second of minute; 0 – 59
10	9	nsceil	Wind Vector Cell (WVC) number 1 – 48
11	10	nslat	Latitude in decimal degrees
12	11	nslon	Longitude in decimal degrees east
13	12	dist	distance between WVC and buoy in km
14	13	ascdes	Asc/Des flag 0 - Ascending pass 1 - Descending pass
15	14	numbeamfore	Number of $\sigma_o$ measurements from fore-beam
16	15	numbeammidv	Number of $\sigma_o$ measurements from mid-V beam
17	16	numbeammidh	Number of $\sigma_o$ measurements from mid-H beam
18	17	numbeamft	Number of $\sigma_o$ measurements from aft beam
19	18	namb	Number of ambiguities; 1 – 4
20	19	numgoodsigma0	The number of $\sigma_o$ 's usable for wind
21	20	qual	WVC quality flag (See NSCAT User's manual)
22	21	mnsdpd	Mean wind speed of all ambiguities ( $\text{ms}^{-1}$ )
23	22	nsmag1	Wind speed for selected ambiguity ( $\text{ms}^{-1}$ )
24	23	nsmagerr1	Wind speed error for selected ambiguity ( $\text{ms}^{-1}$ )
25	24	nsdir1	Wind direction ( $^{\circ}$ ) clockwise from North (oceanographic convention)
26	25	nsdirerr1	Wind direction error ( $^{\circ}$ )
27–30	26–29	Same as 22–25 for ambiguity 2	
31–34	30–33	Same as 22–25 for ambiguity 3	
35–38	34–37	Same as 22–25 for ambiguity 4	

Table 3: NSCAT co-located data parameters.

### 3.2 Co-location

Column	Offset	Name	Description
$\sigma_o$ cells			
39	1	sig0az1	Cell Azimuth (°Clockwise from north) for cell 1
40	2	sig0lat1	Cell latitude (°) for cell 1
41	3	sig0lon1	Cell longitude (°) east for cell 1
42	4	sig0incl	Incidence angle (°) at cell 1
43	5	sig01	$\sigma_o$ in dB for cell 1
44	6	sig0qual1	$\sigma_o$ quality flag (See manual)
45–50	7–12	Same as 1–6 for cell 2	
51–56	13–18	Same as 1–6 for cell 3	
57–62	19–24	Same as 1–6 for cell 4	
63–68	25–30	Same as 1–6 for cell 5	
69–74	31–36	Same as 1–6 for cell 6	

Table 4: NSCAT co-located  $\sigma_o$  parameters.

Column	Offset	Name	Description
Buoy information at hour "n" (prior to NSCAT time)			
294	1	buoyyr	Year; <i>e.g.</i> 1996
295	2	buoymo	Month of year; 1–12
296	3	buoydy	Day of month; 1 – 31
297	4	buoyhr	Hour of day; 0 – 23
298	5	buoymn	Minute of hour; 0 – 59
299	6	buoylat	Latitude in decimal degrees
300	7	buoylon	Longitude in decimal degrees east
301	8	buoyanht	Anemometer height (m)
302	9	buoyTht	Temperature/humidity sensor height (m)
303	10	buoymag	Wind speed ( $\text{ms}^{-1}$ )
304	11	buoydir	Wind direction clockwise from North (oceanographic convention)
305	12	buoyAT	Air Temperature $^{\circ}\text{C}$
306	13	buoySST	Sea Surface Temperature $^{\circ}\text{C}$
307	14	buoy RH	Relative humidity %
308	15	buoyrainp	Percent of 30-second bins that had rain
309	16	buoyrainrate	Average (mm/hour)
310	17	buoyrainstd	Standard deviation of rain rate
311	18	buoyrainmax	Maximum rate during 30-second bins
312	19	buoymag10m	Computed 10 m wind speed $\text{ms}^{-1}$
313	20	depth1	Depth of first mechanical current meter (10 m)
314	21	current1 mag	Magnitude of 10 m current ( $\text{cm s}^{-1}$ )
315	22	current1 dir	Direction of 10 m current (degrees)
316	23	depth1	Depth of second mechanical current meter (25 m)
317	24	current2 mag	Magnitude of 25 m current ( $\text{cm s}^{-1}$ )
318	25	current2 dir	Direction of 25 m current (degrees)
319	26	depth1	Depth of third mechanical current meter (30 m)
320	27	current3 mag	Magnitude of 30 m current ( $\text{cm s}^{-1}$ )
321	28	current3 dir	Direction of 30 m current (degrees)
322–349	29–56	Buoy information at hour "n+1" (following NSCAT time)	

Table 5: Buoy Co-located data parameters.

## 4 Wind Comparisons

Comparisons of ocean winds between the NASA scatterometer and the buoys were made using statistical methods derived from Graber *et al.* (1996) and Freilich and Dunbar (1999). The statistics used by Graber *et al.* include a symmetrical regression, instead of a linear regression, since the error characteristics of the buoy and scatterometer are not known *a priori* (Freilich 1997). The symmetrical regression does not require the dependence of either the buoy or scatterometer measurement. Freilich and Dunbar (1999) have suggested a single scalar quantity to determine the accuracy of scatterometer wind velocity measurements: a vector correlation statistic ( $\rho^2$ ) of two vector time series, as proposed in Crosby *et al.* (1993). The vector correlation is equal to zero if the two vector time series are independent and is equal to two if they are perfectly correlated. Both comparisons are included since each one provides insight into the characteristics of the scatterometer.

Before the comparisons were made, each co-location was checked for erroneous or missing data. Co-locations were kept if the buoy record reported a valid wind and valid air and sea surface temperature. Estimates for relative humidity and atmospheric pressure were used if actual measurements were not available. In addition, only the WVCs with a "WVC\_Quality\_Flag" of 0 are used: which means that all  $\sigma_o$ 's are used and there is no land/ice contamination. Although the co-location file contains the four closest pairs within 100 km and 1 hr, only the closest pairs that were within one WVC (25 km or 50 km) and 30 minutes were used in the analysis.

For each co-located scatterometer datum  $S$  and buoy datum  $B$  the following statistics were computed on 10 m wind speed and direction:

Bias (scatterometer - buoy)	$\langle S - B \rangle$
Root-mean-square error (RMSE)	$\langle (S - B)^2 \rangle^{1/2}$
Correlation Coefficient	$\frac{\langle (S - \bar{S})(B - \bar{B}) \rangle}{\langle (S - \bar{S})^2 \rangle^{1/2} \langle (B - \bar{B})^2 \rangle^{1/2}}$
Slope of symmetrical regression	$\tan \xi = (\langle S^2 \rangle / \langle B^2 \rangle)^{1/2}$

The next two statistics were computed for the wind directions only. The oceanographic convection was used where wind "toward the North" is defined as  $0^\circ$  and wind "toward the East" is define as  $90^\circ$ .

Mean angular difference	$\Delta\theta = \tan^{-1} \left[ \frac{\langle \sin(\theta_S - \theta_B) \rangle}{\langle \cos(\theta_S - \theta_B) \rangle} \right]$
Standard deviation of angular difference	$\sigma_\theta = \sin^{-1}(\epsilon) [1 + 0.1547\epsilon^3]$

with  $\epsilon$  defined by Yamartino (1984) as

$$\epsilon = \sqrt{1 - [(\sin \Delta\theta)^2 + (\cos \Delta\theta)^2]}$$

$$\sin \Delta\theta = \langle \sin(\theta_S - \theta_B) \rangle$$

$$\cos \Delta\theta = \langle \cos(\theta_S - \theta_B) \rangle$$

and where  $\langle \rangle$  represents the mean.

The vector correlation statistic ( $\rho^2$ ) from Freilich and Dunbar (1999) is defined as follows,

$$\rho^2 \equiv Tr [(\Sigma_{11})^{-1} \Sigma_{12} (\Sigma_{22})^{-1} \Sigma_{21}]$$

where  $\Sigma_{ab}$  is the  $2 \times 2$  cross-covariance matrix for the co-located wind vector time series  $a$  and  $b$ .

#### 4.1 Instrument accuracies

The following table lists the instrument specifications for wind speed and direction. The accuracies of the TAO winds are determined at PMEL by pre and post deployment calibrations over a typical year long deployment using 198 pre/post deployment comparisons. The WHOI IMET (Hosom, 1993) and VAWR (Weller, 1989) were not calibrated prior to this intercomparison. However, the short 3 month overlap should not be affected by long term instrument drift.

Instrument	Parameter	Accuracy	Range
NSCAT	speed	2 ms <sup>-1</sup> (rms) 10%	3–20 ms <sup>-1</sup> 20–30 ms <sup>-1</sup>
	direction	20°(rms) (closest ambiguity)	3–30 ms <sup>-1</sup>
TAO	speed	greater of 0.3 ms <sup>-1</sup> or 3%	0–20 ms <sup>-1</sup>
	direction	+/- 5°	0–360°
WHOI IMET	speed	greater of 0.2 ms <sup>-1</sup> or 2%	0.7–50 ms <sup>-1</sup>
	direction	2.8°(rms)	0–360°
WHOI VAWR	speed	or 2%	2–20 ms <sup>-1</sup>
	direction	3°(rms)	0–360°

Table 6: Instrument accuracies.

## 4.2 TAO wind comparisons

There are 5580 co-located pairs of TAO and 25 km NSCAT-1 winds, 5196 pairs of TAO and 50 km NSCAT-1, and 6334 pairs of TAO and 25 km NSCAT-2 winds available from ten months of NSCAT data. The difference in the number of co-locations was due to a combination of additional TAO winds and the scatterometer model function. Scatterplots of TAO vs. NSCAT (25 km) wind speed and direction are shown in figure 5. The statistics listed above are detailed in table 7. The 50 km data set produces slightly better results than the 25 km data set. Significant improvement is seen in the 25 km NSCAT-2 data. The statistics are binned by wind speed to isolate any dependences on the wind speed. The wind speed ranges are binned based on the buoy wind speed. Most of the winds ( $\sim 94\%$ ) were less than  $10 \text{ ms}^{-1}$  and a significant number ( $\sim 27\%$ ) were less than  $5 \text{ ms}^{-1}$ .

The RMSE for the wind speed for the NSCAT-1 25 km and 50 km data sets is  $1.45 \text{ ms}^{-1}$  and  $1.52 \text{ ms}^{-1}$  respectively. This is improved to  $1.31 \text{ ms}^{-1}$  for the NSCAT-2 25 km winds. The smaller NSCAT-2 RMSE is seen in all wind speed bins. The smallest RMSE is in the  $7.5\text{--}10 \text{ ms}^{-1}$  wind speed range; and largest in the  $0\text{--}5 \text{ ms}^{-1}$  if the  $12.5\text{--}50 \text{ ms}^{-1}$  range is omitted due to the small sample size. The bias and RMSE is influenced by large scatterometer overestimates of wind speed. Eliminating co-locations where the scatterometer overestimates the buoy winds by more than  $3 \text{ ms}^{-1}$  (NSCAT-2) changes the bias from  $-0.07 \text{ ms}^{-1}$  to  $-0.20 \text{ ms}^{-1}$  and the RMSE from  $1.30 \text{ ms}^{-1}$  to  $0.93 \text{ ms}^{-1}$ .

The symmetrical regression coefficient for the NSCAT-1 co-location sets is about 0.93. This value is nearly constant in all ranges of wind speeds, except in the lowest and highest wind speeds. This is improved to 1.00 for the NSCAT-2 winds.

The mean angular difference between the TAO wind vector and the NSCAT wind vector is in general about  $10^\circ$ . The NSCAT winds are, in the mean, clockwise from the TAO winds and are not improved with the NSCAT-2 model function. The direction bias is not speed dependent, but the standard deviation of the difference is large for wind speeds less than  $5 \text{ ms}^{-1}$ .

The vector correlation  $\rho^2$  is about 1.4 for each NSCAT wind product over all wind speeds. The winds are not very well correlated at low wind speed, but are reasonably well correlated above  $7.5 \text{ ms}^{-1}$ . The best correlation occurs in the  $7.5\text{--}10.0 \text{ ms}^{-1}$  wind speed bin. Vector correlation improves only marginally for the NSCAT-2 co-locations indicating that directional bias affects the correlation more than the speed bias.



The wind speeds (left panel) and directions (right panel) binned in  $1.0 \text{ ms}^{-1}$  and  $30^\circ$  bins are shown in figures 6–8. The number of co-located pairs are shown in the lower panels of these figures. Although the number of co-locations has a gaussian shape about  $7 \text{ ms}^{-1}$  for wind speed, the cluster of wind directions between  $180^\circ$  and  $360^\circ$  shows the predominant westward wind direction in the tropical Pacific. The NSCAT-1 25 km and 50 km winds are very similar up to about  $12 \text{ ms}^{-1}$ . The wind speed improvements in the NSCAT-2 winds was distributed over the  $4\text{--}11 \text{ ms}^{-1}$  wind speed range.

## 4.2 TAO wind comparisons

Table 7: Comparison of NSCAT wind speeds and directions with TAO buoy 10 m winds. See section 4.2 for a discussion of the results.

Product	Wind Speed Range $\text{ms}^{-1}$	Sample Size	Wind Speed				Wind Direction		Vector Correlation $\rho^2$
			Bias $\text{ms}^{-1}$	RMSE $\text{ms}^{-1}$	Correlation Coefficient	Symmetrical Regression	Bias (deg)	Std. D. (deg)	
NSCAT-1 25 km	0.0 – 50.0	5580	-0.54	1.45	0.85	0.93	9.78	33.43	1.41
	0.0 – 5.0	1523	-0.16	1.68		1.03	8.78	55.31	0.60
	5.0 – 7.5	2082	-0.61	1.41		0.92	10.53	25.86	1.30
	7.5 – 10.0	1634	-0.71	1.18		0.92	9.73	17.80	1.59
	10.0 – 12.5	312	-0.83	1.51		0.93	8.26	22.20	1.52
NSCAT-1 50 km	12.5 – 50.0	29	-2.63	3.62		0.82	11.92	22.32	1.58
	0.0 – 50.0	5196	-0.45	1.52	0.83	0.94	8.85	32.57	1.44
	0.0 – 5.0	1444	0.03	1.91		1.11	7.82	54.35	0.62
	5.0 – 7.5	1887	-0.53	1.35		0.94	9.14	25.20	1.33
	7.5 – 10.0	1550	-0.71	1.19		0.92	9.41	15.69	1.64
NSCAT-2 25 km	10.0 – 12.5	294	-0.77	1.62		0.94	7.25	20.36	1.57
	12.5 – 50.0	21	-2.40	3.52		0.84	12.06	19.87	1.58
	0.0 – 50.0	6334	-0.07	1.30	0.86	1.00	10.03	32.90	1.46
	0.0 – 5.0	1796	0.22	1.59		1.13	9.80	54.12	0.73
	5.0 – 7.5	2353	-0.11	1.16		1.00	10.48	25.20	1.37
	7.5 – 10.0	1844	-0.23	1.09		0.98	9.81	16.66	1.62
	10.0 – 12.5	317	-0.36	1.40		0.97	8.76	20.27	1.56
	12.5 – 50.0	24	-1.80	2.94		0.88	13.16	20.13	1.50

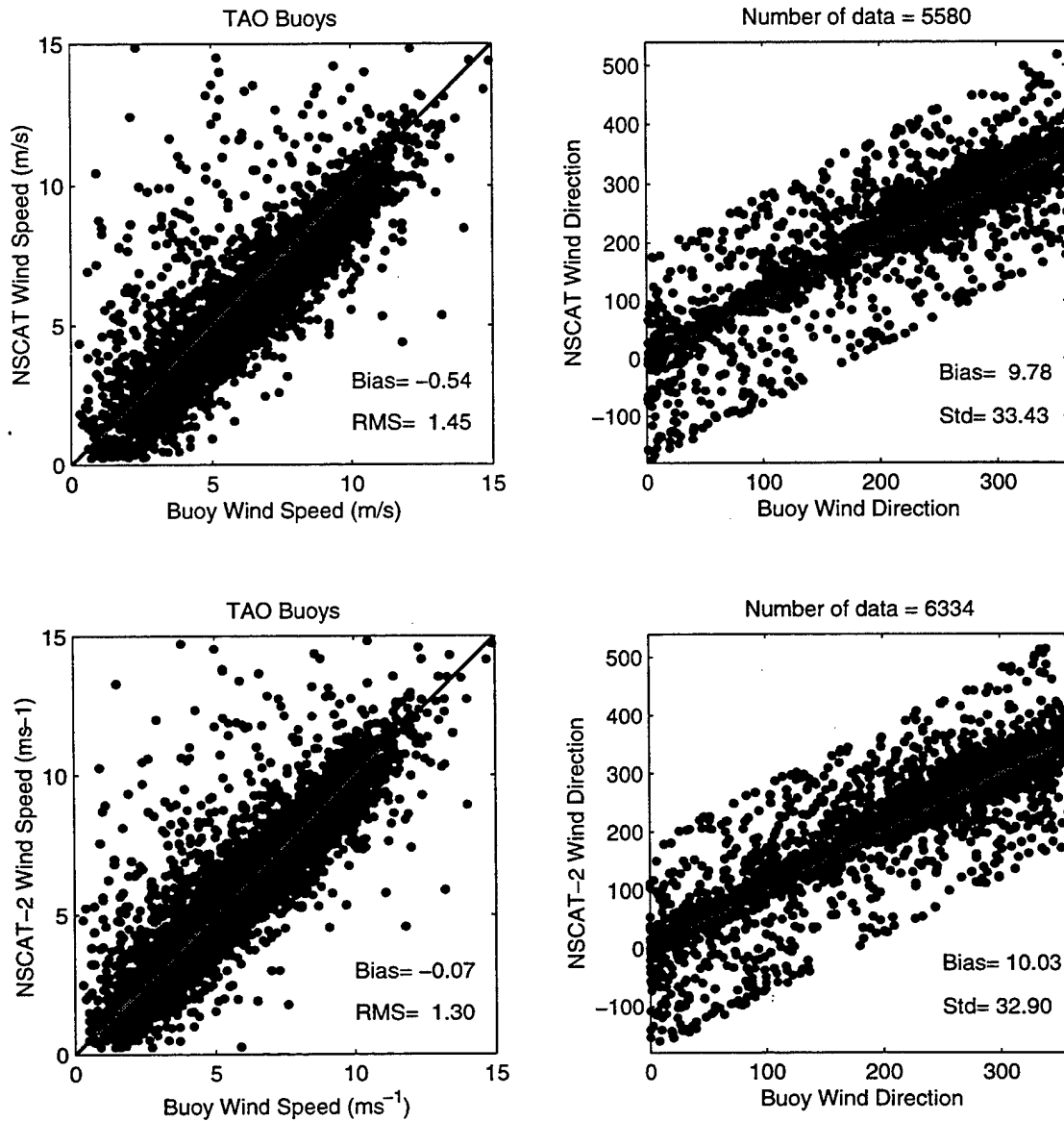


Figure 5: Scatterplots of wind speeds and directions derived from 25 km high resolution winds from NSCAT-1 (top) and NSCAT-2 (bottom) model functions with TAO 10 m buoy winds. Both wind products show similar results, however, the NSCAT-2 results have a lower speed bias and RMS error.

## 4.2 TAO wind comparisons

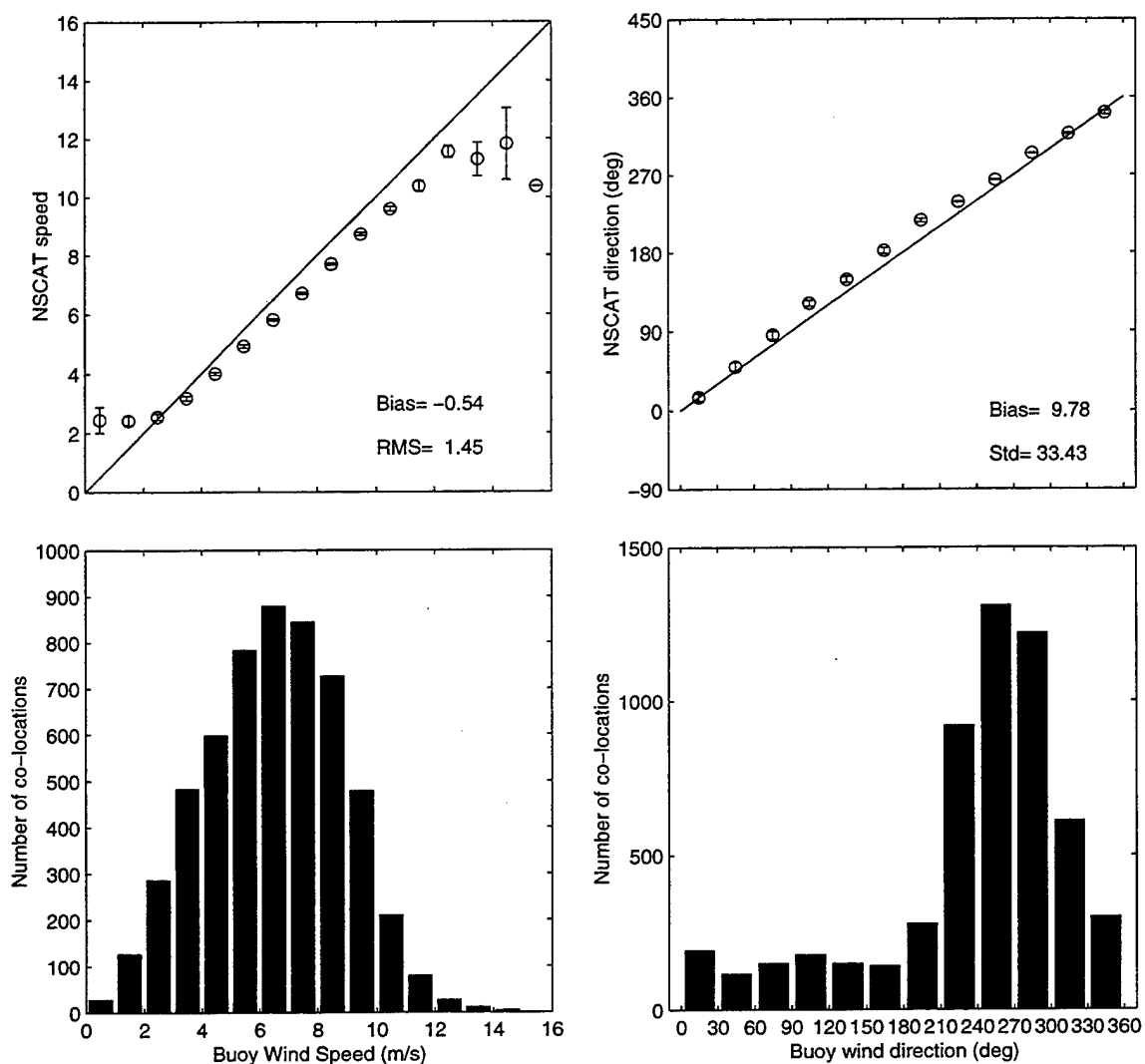


Figure 6: NSCAT-1 25 km high resolution wind speeds and directions binned against TAO 10 m buoy winds. The top figure shows the wind speed and directions binned in  $1.0 \text{ ms}^{-1}$  and  $30^\circ$  bins. The error bars show the estimated error in each bin. The bottom figure shows the distribution of co-locations in each bin.

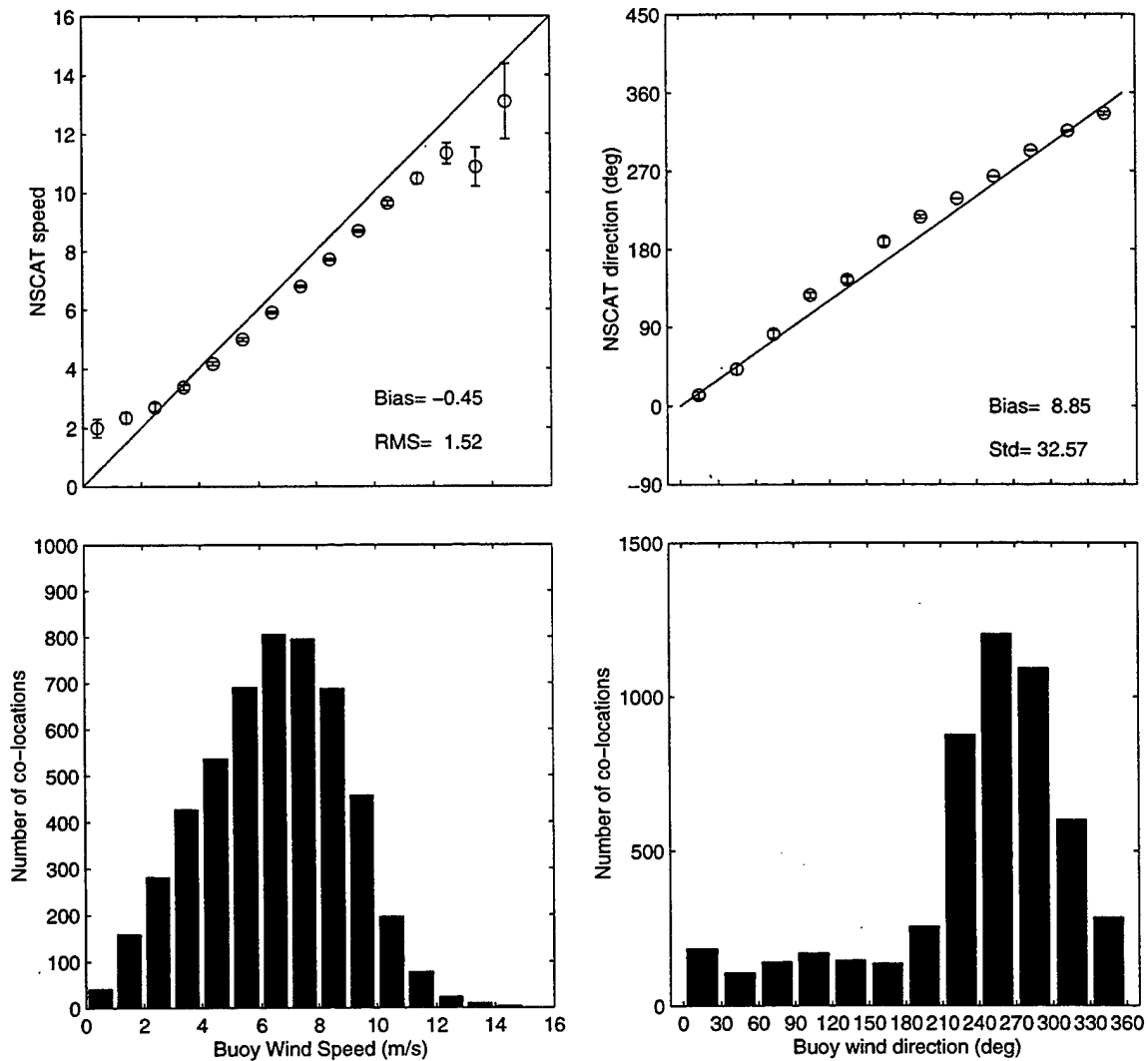


Figure 7: Same as for figure 6, except for NSCAT-1 50 km standard winds.

## 4.2 TAO wind comparisons

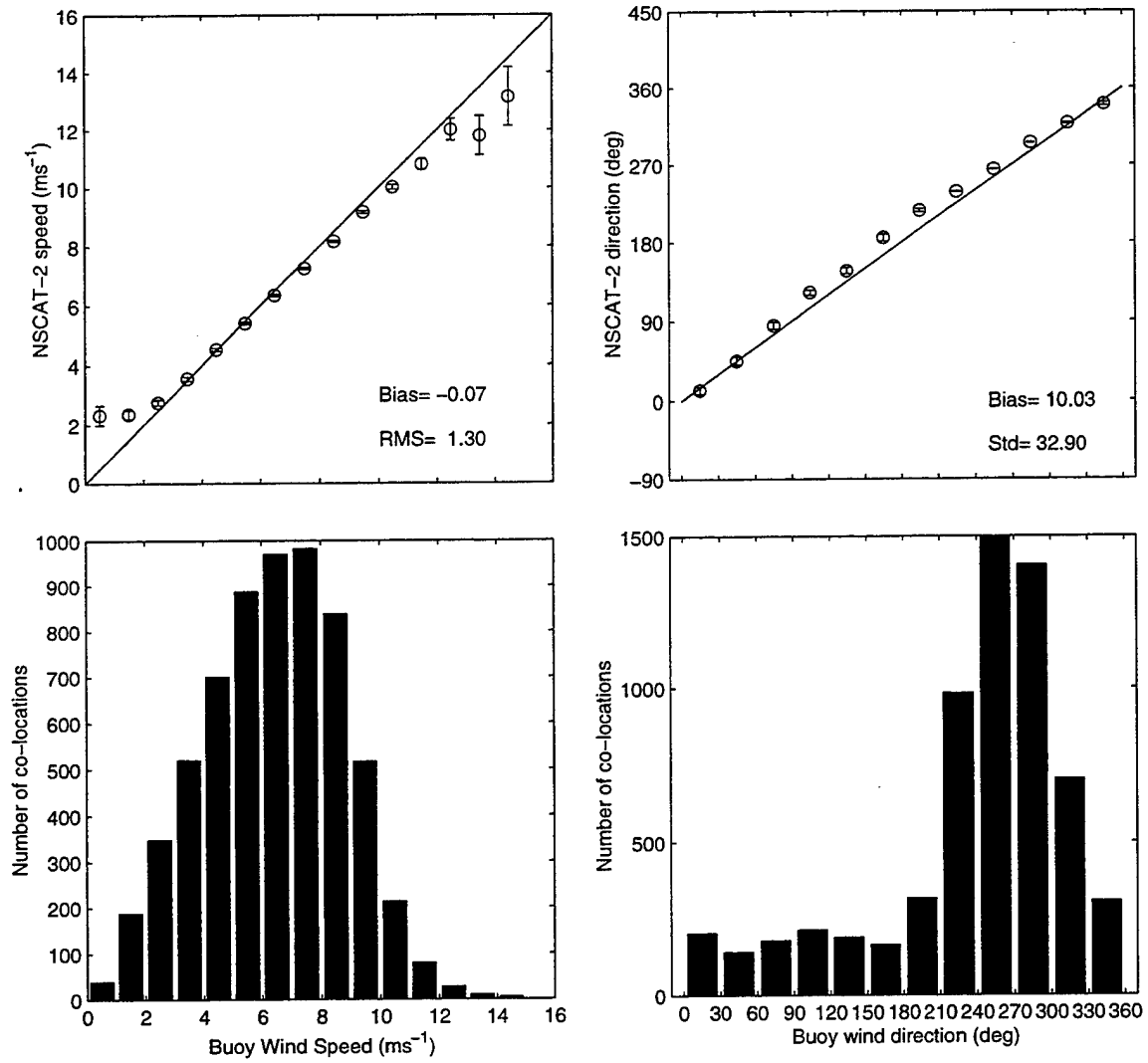


Figure 8: Same as for figure 6, except for NSCAT-2 25 km standard winds.

### 4.3 Interpretation of the speed bias

Overall, the ensemble NSCAT-2 wind speed bias, as shown above, is about  $-0.1 \text{ ms}^{-1}$ . However, this straight difference method for determining the bias of a vector magnitude is misleading. As discussed in detail in Freilich (1997), the fact that speed must be non-negative means that the errors are not normally distributed about the mean speed. This results in a bias that is skewed towards the positive, particularly at the low wind speeds.

To see this, we derive a speed bias estimate for the case where there is no bias in the wind components,  $(u, v)$ . Let  $\vec{u}_b = (u_b, v_b)$  be the buoy wind vector,  $\vec{u}_s = (u_s, v_s)$  be the scatterometer wind vector and  $s = [u^2 + v^2]^{\frac{1}{2}}$  be the wind speed. Assume that the buoys have no errors, but the scatterometer has errors  $\epsilon$ , relative to the buoy, so that  $\vec{u}_s = (u_b + \epsilon_{u_s}, v_b + \epsilon_{v_s})$ . The means of the component errors are zero. Speed then becomes  $s_s^2 = [u_b^2 + 2u_b\epsilon_{u_s} + \epsilon_{u_s}^2 + v_b^2 + 2v_b\epsilon_{v_s} + \epsilon_{v_s}^2]$ . Assume that errors do not depend on wind speed or  $\langle u_b\epsilon_{u_s} \rangle = \langle v_b\epsilon_{v_s} \rangle = 0$ , where  $\langle \cdot \rangle$  is the expected value. Then

$$\begin{aligned} \langle s_s^2 - s_b^2 \rangle &= \langle [s_b^2 + 2u_b\epsilon_{u_s} + 2v_b\epsilon_{v_s} + \epsilon_{u_s}^2 + \epsilon_{v_s}^2] - s_b^2 \rangle, \\ &= \langle \epsilon_{u_s}^2 \rangle + \langle \epsilon_{v_s}^2 \rangle \end{aligned}$$

If  $\langle \epsilon_{u_s}^2 \rangle \sim \langle \epsilon_{v_s}^2 \rangle \equiv \epsilon_0^2$ , then  $\langle s_s^2 - s_b^2 \rangle = 2\epsilon_0^2$ , where the apparent bias  $b = s_s - s_b$ . This bias  $b$  is an artifact of using speed for the comparisons and is a measure of the root-mean-square error between wind components, rather than a true bias.

Figure 9 shows the wind speed bias for NSCAT-1 (o) as a function of the TAO wind speeds. The bias goes up drastically at low winds speeds. To get a better estimate of the true bias, we compared wind components. The zonal and meridional components for the TAO buoys and NSCAT (NSCAT-1 on the left) are plotted in Figure 10. The wind vectors were used in this plot only if the TAO and NSCAT wind directions were within  $30^\circ$ . Also, only the larger component of each vector was included. The slopes of the best linear fit are 0.92 and 0.93 for the zonal and meridional components, respectively, for the NSCAT-1 comparison and increase to 0.97 and 1.01 for the NSCAT-2 components. These numbers suggest that the NSCAT-1 model function has a gain problem more so than a bias problem. The gain for NSCAT-1, 0.925, is shown with the solid line in Figure 9. Subtracting this gain from the NSCAT-1 wind speed bias gives the dashed line. The dashed line is representative of an artificial bias in the wind speed bias. The artificial bias is near zero for most of the speed range, but has a large positive value at the low wind speeds, reflecting the fact that the errors cannot vary symmetrically about the wind speed. The small negative values in the remainder of the dashed curve result from the gain being determined from a filtered data set compared to that used to compute the speed bias.

### 4.3 Interpretation of the speed bias

---

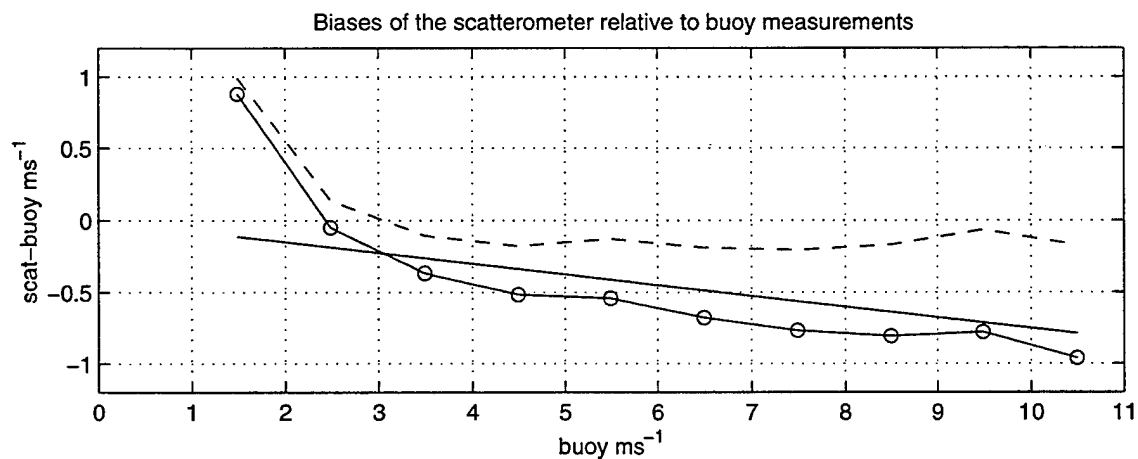


Figure 9: Biases of scatterometer winds relative to buoy measurements. Bias of NSCAT-1 wind speed compared to the co-located TAO wind speeds shown with circles. The solid line has a slope of 0.925 showing the gain problem between NSCAT-1 and TAO. Subtracting the gain from the wind speed bias gives the dashed line, representing the artificial bias incurred when computing a wind speed bias.



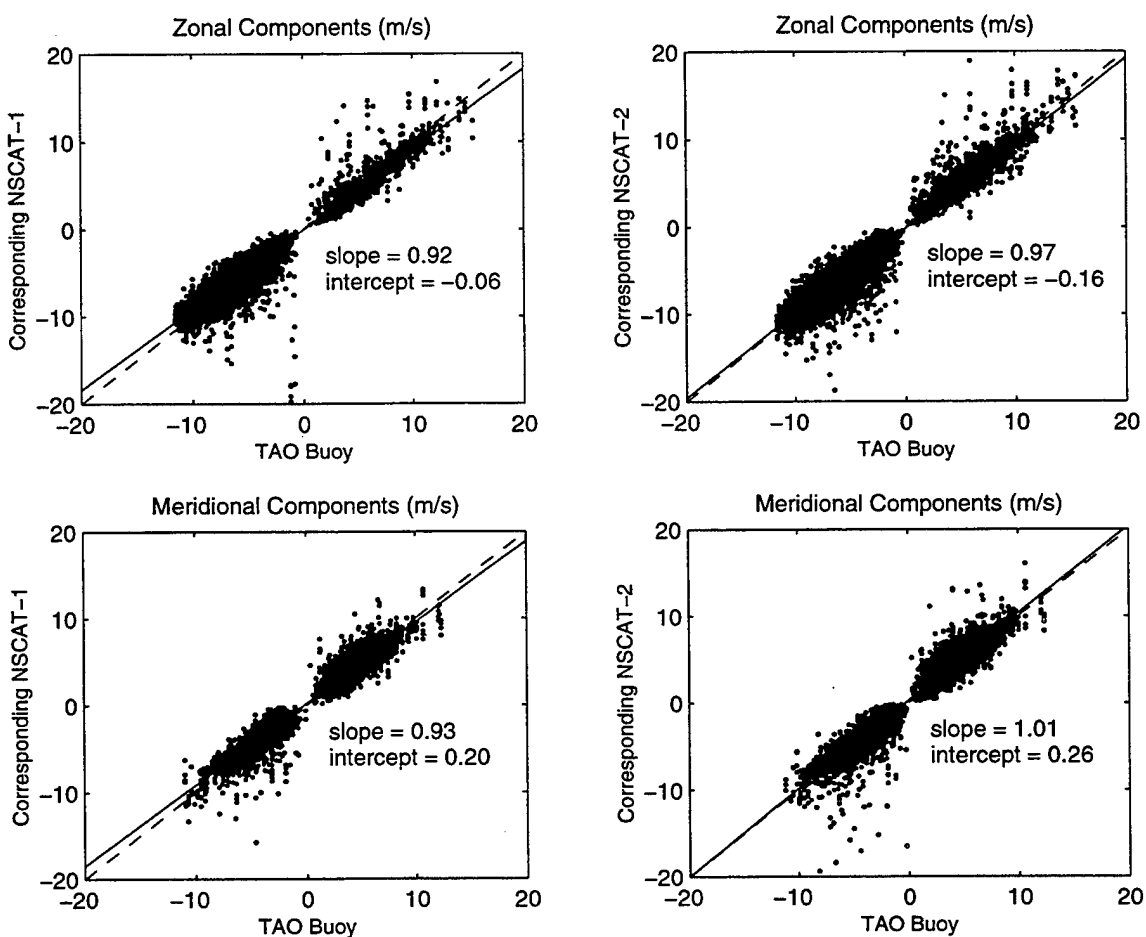


Figure 10: a) Zonal and b) meridional component scatterplots of TAO buoy and NSCAT winds. Dashed line is best linear fit, solid is one-to-one correspondence. See text for details.

## 4.4 WHOI wind comparisons

Since the two WHOI buoys, located along 125°W, contain two separate meteorological packages, three comparisons are made: a) all co-locations (table 8); b) IMET only (table 9) and c) VAWR only (table 10).

### 4.4.1 Combined IMET and VAWR winds

The combined winds include all buoy measurements that fit the co-location criteria for each WVC (table 8). Due to the reporting intervals of the IMET (hourly) and VAWR (15-minute), up to 5 co-locations may occur. Analysis of the closest IMET or VAWR is given in the following sections.

The wind speed biases for both the 25 km and 50 km data sets are not as large for the combined WHOI winds as they are for the TAO winds. However, they are still negative at about  $-0.3 \text{ ms}^{-1}$  for all NSCAT-1 wind speeds. The NSCAT-2 wind speed biases are slightly positive ( $0.06 \text{ ms}^{-1}$ ). These biases also follow the same trend as those with the TAO data, in that they are positive for the lowest wind speed range (as expected *cf.* figure 9) and go increasingly more negative in the higher wind speed ranges. The root mean square errors and the slope of symmetrical regression parameters are also best in the mid-speed range and get worse at the extremes.

The wind direction biases of the scatterometer compared to the combined WHOI buoy data are smaller than the direction biases with the TAO data and of the opposite sign: the scatterometer winds are to the left or counter-clockwise from the WHOI winds (figure 11). The standard deviations of the direction differences are highest at the low wind speeds, similar to those in the TAO comparisons.

The vector correlation coefficients are lower for the WHOI winds than the TAO winds except in the  $7.5\text{--}12.5 \text{ ms}^{-1}$  range for the 25 km NSCAT winds but overall are the same. The 25 km NSCAT-1 wind product is similar in speed, but slightly better in direction, than the 50 km winds. The  $7.5\text{--}10.0 \text{ ms}^{-1}$  range shows excellent agreement with a vector correlation of 1.71, RMS error of  $0.97 \text{ ms}^{-1}$  and standard deviation of direction difference of  $13.45^\circ$ . The wind directions have a smaller bias than the TAO buoys, but have similar standard deviations.

Table 8: Comparison of NSCAT wind speeds and directions with WHOI buoy 10 m winds. See section 4.4.1 for a discussion of the results.

Product	Wind Speed Range $\text{ms}^{-1}$	Sample Size	Wind Speed				Wind Direction		Vector Correlation $\rho^2$
			Bias $\text{ms}^{-1}$	RMSE $\text{ms}^{-1}$	Correlation Coefficient	Symmetrical Regression	Bias (deg)	Std. D. (deg)	
NSCAT-1 25 km	0.0 – 50.0	366	-0.35	1.38	0.82	0.94	-3.38	31.27	1.32
	0.0 – 5.0	87	0.56	1.85		1.21	-1.64	49.31	0.47
	5.0 – 7.5	127	-0.58	0.96		0.92	-8.57	32.72	1.02
	7.5 – 10.0	142	-0.53	0.97		0.94	-0.08	13.45	1.71
NSCAT-1 50 km	10.0 – 12.5	10	-2.79	3.79		0.76	-3.65	7.38	1.58
	0.0 – 50.0	294	-0.22	1.34	0.81	0.96	-4.87	40.21	0.90
	0.0 – 5.0	71	0.66	1.82		1.24	-10.68	66.61	0.55
	5.0 – 7.5	113	-0.40	0.93		0.95	-5.00	26.25	0.83
NSCAT-2 25 km	7.5 – 10.0	108	-0.54	1.02		0.94	-2.45	33.43	1.10
	10.0 – 12.5	2	-4.99	6.40		0.62	-7.14	4.78	N/A
	0.0 – 50.0	271	0.06	1.13	0.87	0.99	-5.13	29.26	1.46
	0.0 – 5.0	67	0.88	1.61		1.27	-15.28	53.80	0.45
	5.0 – 7.5	101	-0.09	0.68		0.99	-6.47	17.71	1.31
	7.5 – 10.0	99	-0.24	0.79		0.97	0.78	14.87	1.71
	10.0 – 12.5	4	-2.49	3.90		0.79	-6.06	6.37	1.15

#### 4.4 WHOI wind comparisons

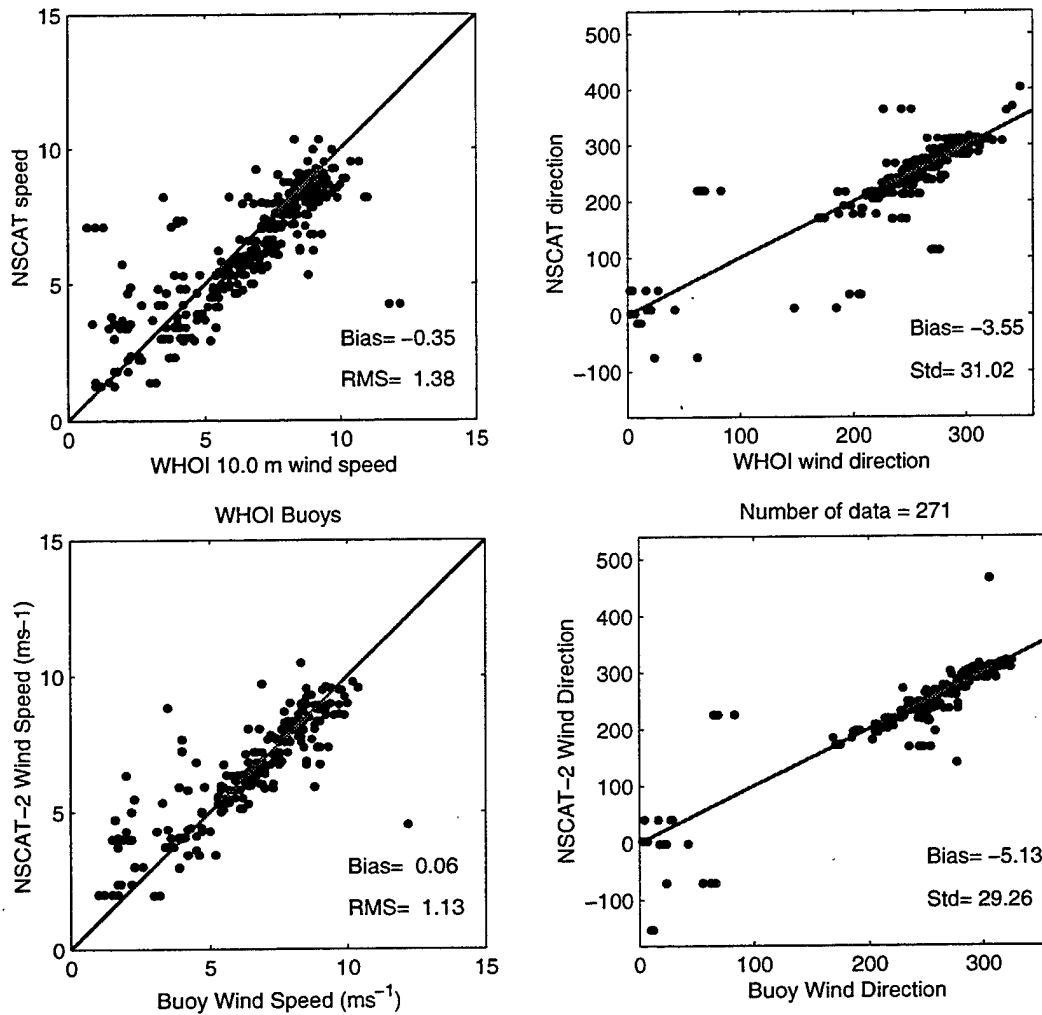


Figure 11: Scatterplots of wind speeds and directions derived from 25 km high resolution winds NSCAT-1 (top) and NSCAT-2 (bottom) with WHOI 10 m buoy winds. The wind speed comparisons are similar to the TAO comparisons with an overall negative bias with the NSCAT-2 winds closer to the buoy winds. The wind directions differ from TAO with a negative bias, but are similar to TAO with both model functions producing similar biases.

#### 4.4.2 IMET winds

The sampling interval for the IMET measurements was 1 minute and the averaging/reporting interval was 1 hour. The NSCAT-1 winds show good agreement with the WHOI IMET winds in the mid-speed range ( $5\text{--}10\text{ ms}^{-1}$ ), but show a large positive bias (scatterometer winds higher than the WHOI IMET winds) of almost  $1\text{ ms}^{-1}$  at low wind speeds (table 8). The comparisons in the  $7.5\text{--}10\text{ ms}^{-1}$  range, are very good in all categories. The NSCAT-2 winds show the same ( $0.4\text{--}0.5\text{ ms}^{-1}$ ) bias shift seen in TAO and WHOI VAWR comparisons with the lower wind speed bins showing the highest shift.

Overall, the 25 km data set compares slightly better than the 50 km winds. In the  $7.5\text{--}10\text{ ms}^{-1}$  range, the vector correlation, wind speed bias, RMS error and direction error are 1.81, 0.08, 0.64 and 9.73. These values for the NSCAT-2 winds of 1.87, 0.37, 0.68 and 8.08 are similar except for the bias. There were no co-locations for buoy wind speeds greater than  $10\text{ ms}^{-1}$ . The scatterplots in figure 11, show the slight positive wind speed biases, as well as the predominately westward winds.

The wind directions show very little direction bias. The values are between  $1^\circ$  and  $4^\circ$  clockwise with respect to the scatterometer winds for both the 25 km and 50 km winds. There seem to be very few flipped (directional differences greater than  $120^\circ$ ) vectors, although the data set is small.

Table 9: Comparison of NSCAT wind speeds and directions with WHOI buoy IMET 10 m winds. See section 4.4.2 for a discussion of the results.

Product	Wind Speed Range $\text{ms}^{-1}$	Sample Size	Wind Speed				Wind Direction		Vector Correlation $\rho^2$
			Bias $\text{ms}^{-1}$	RMSE $\text{ms}^{-1}$	Correlation Coefficient	Symmetrical Regression	Bias (deg)	Std. D. (deg)	
NSCAT-1 25 km	0.0 – 50.0	101	0.13	1.12	0.86	1.02	-1.40	28.46	1.35
	0.0 – 5.0	25	0.88	1.81		1.30	2.37	43.62	0.66
	5.0 – 7.5	39	-0.29	0.88		0.96	-4.28	29.46	1.24
	7.5 – 10.0	37	0.08	0.64		1.01	-0.63	9.73	1.81
NSCAT-1 50 km	0.0 – 50.0	85	0.17	1.11	0.85	1.02	-1.27	33.37	1.03
	0.0 – 5.0	18	0.95	1.83		1.31	-1.14	59.60	0.96
	5.0 – 7.5	37	-0.16	0.93		0.98	-2.83	24.24	1.06
	7.5 – 10.0	30	0.11	0.64		1.02	0.60	23.76	1.16
NSCAT-2 25 km	0.0 – 50.0	78	0.58	1.24	0.86	1.07	-2.32	22.95	1.52
	0.0 – 5.0	20	1.52	2.12		1.48	-9.29	42.78	0.71
	5.0 – 7.5	32	0.16	0.76		1.03	-2.15	12.34	1.67
	7.5 – 10.0	26	0.37	0.68		1.05	1.56	8.08	1.87

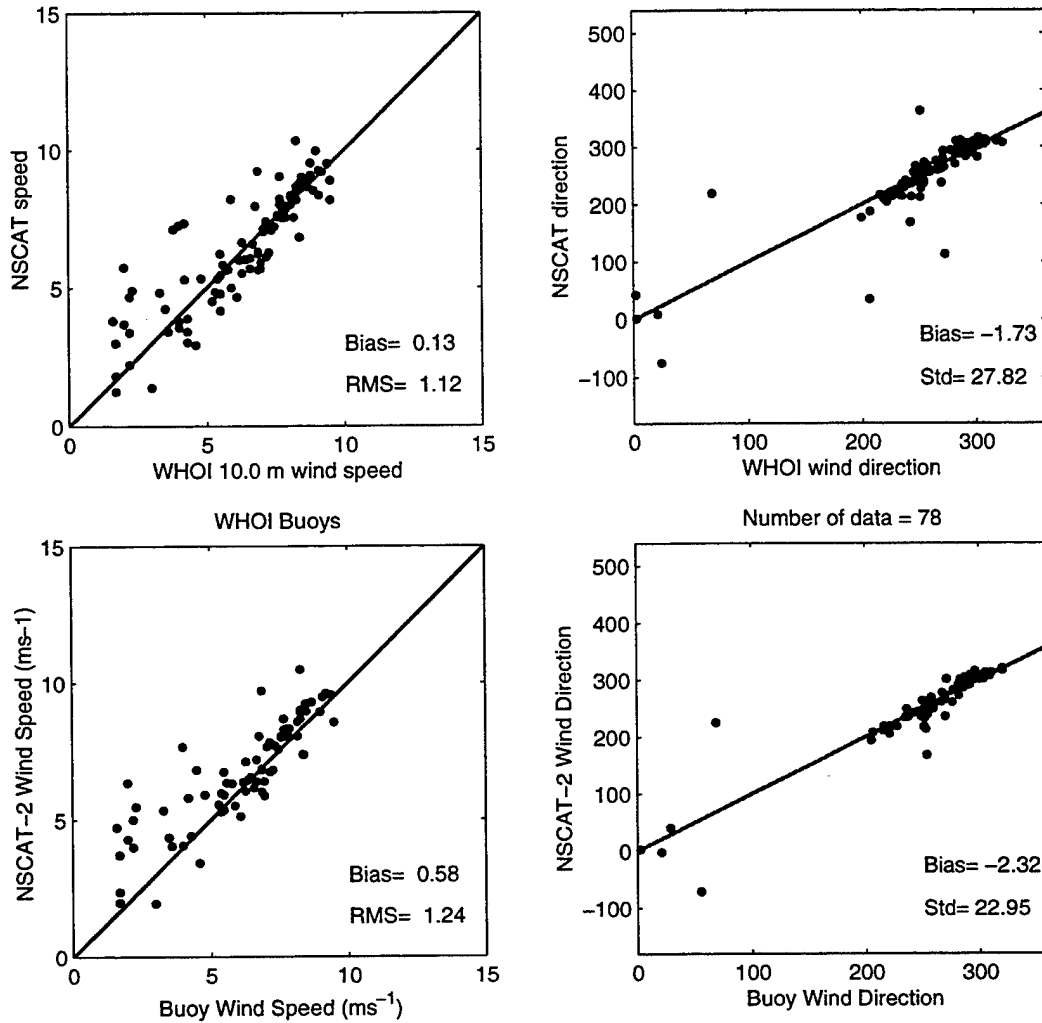


Figure 12: Scatterplots of wind speeds and directions derived from 25 km high resolution winds NSCAT-1 (top) and NSCAT-2 (bottom) with WHOI IMET 10 m buoy winds. This comparison shows an excellent agreement in magnitude for the NSCAT-1 winds and a  $0.6 \text{ ms}^{-1}$  bias for the NSCAT-2 winds. The direction biases are similar for the two model functions.

#### 4.4 WHOI wind comparisons

---

##### 4.4.3 VAWR winds

The sampling interval for the VAWR was 7.5-minutes and the reporting interval was 15-minutes. The 1-hour co-location interval produced multiple VAWR co-locations due to the 15 minute reporting interval. However, only the closest buoy vector in time and space was used for the direct comparison. The VAWR had a temporary malfunction from June 8 to the end of the NSCAT mission. Those records were removed before analysis.

The results of the comparison of NSCAT with the WHOI VAWR are similar to those from the WHOI IMET, except for one main difference. The wind speed bias, which is slightly positive for the IMET data (scatterometer larger than the buoy speeds), is negative by almost  $0.5 \text{ ms}^{-1}$  for the VAWR data. Although the VAWR wind speed biases are similar to those of the TAO data, this bias may be due to the over-speeding of the anemometer cups (Beardsley *et al.*, 1998). In the wind speed scatterplots (figure 13) the negative bias of almost  $0.5 \text{ ms}^{-1}$  is clearly evident. NSCAT-2 winds show the same bias shift seen in the TAO winds. The wind speed statistics are similar for TAO and WHOI VAWR.

The wind direction has a slightly larger bias and standard deviation when comparing scatterometer data with the VAWR data than with the IMET data. Again there is the almost exclusive westward winds in the co-locations.



Table 10: Comparison of NSCAT wind speeds and directions with WHOI buoy VAWR 10 m winds. See section 4.4.3 for a discussion of the results.

Product	Wind Speed Range $\text{ms}^{-1}$	Sample Size	Wind Speed				Wind Direction		Vector Correlation $\rho^2$
			Bias $\text{ms}^{-1}$	RMSE $\text{ms}^{-1}$	Correlation Coefficient	Symmetrical Regression	Bias (deg)	Std. D. (deg)	
NSCAT-1 25 km	0.0 – 50.0	91	-0.49	1.54	0.80	0.92	-3.92	33.32	1.34
	0.0 – 5.0	23	0.44	2.04		1.19	-0.40	57.36	0.46
	5.0 – 7.5	28	-0.69	0.92		0.89	-9.57	33.64	0.99
	7.5 – 10.0	37	-0.67	0.92		0.93	-1.51	8.61	1.87
	10.0 – 12.5	3	-3.38	4.68		0.72	-5.32	6.10	2.00
NSCAT-1 50 km	0.0 – 50.0	92	-0.35	1.65	0.75	0.94	-4.63	38.91	0.92
	0.0 – 5.0	25	0.65	2.03		1.26	-2.96	62.98	0.61
	5.0 – 7.5	29	-0.44	0.92		0.94	-6.42	26.60	1.02
	7.5 – 10.0	36	-0.71	1.06		0.92	-3.71	29.37	1.14
	10.0 – 12.5	2	-4.99	6.40		0.62	-7.14	4.78	N/A
NSCAT-2 25 km	0.0 – 50.0	90	-0.10	1.26	0.84	0.97	-5.41	30.75	1.42
	0.0 – 5.0	24	0.66	1.61		1.22	-12.09	55.99	0.41
	5.0 – 7.5	30	-0.20	0.60		0.97	-7.18	22.84	1.17
	7.5 – 10.0	33	-0.31	0.57		0.96	-0.82	8.79	1.89
	10.0 – 12.5	3	-2.98	4.47		0.76	-6.11	7.36	2.00

#### 4.4 WHOI wind comparisons

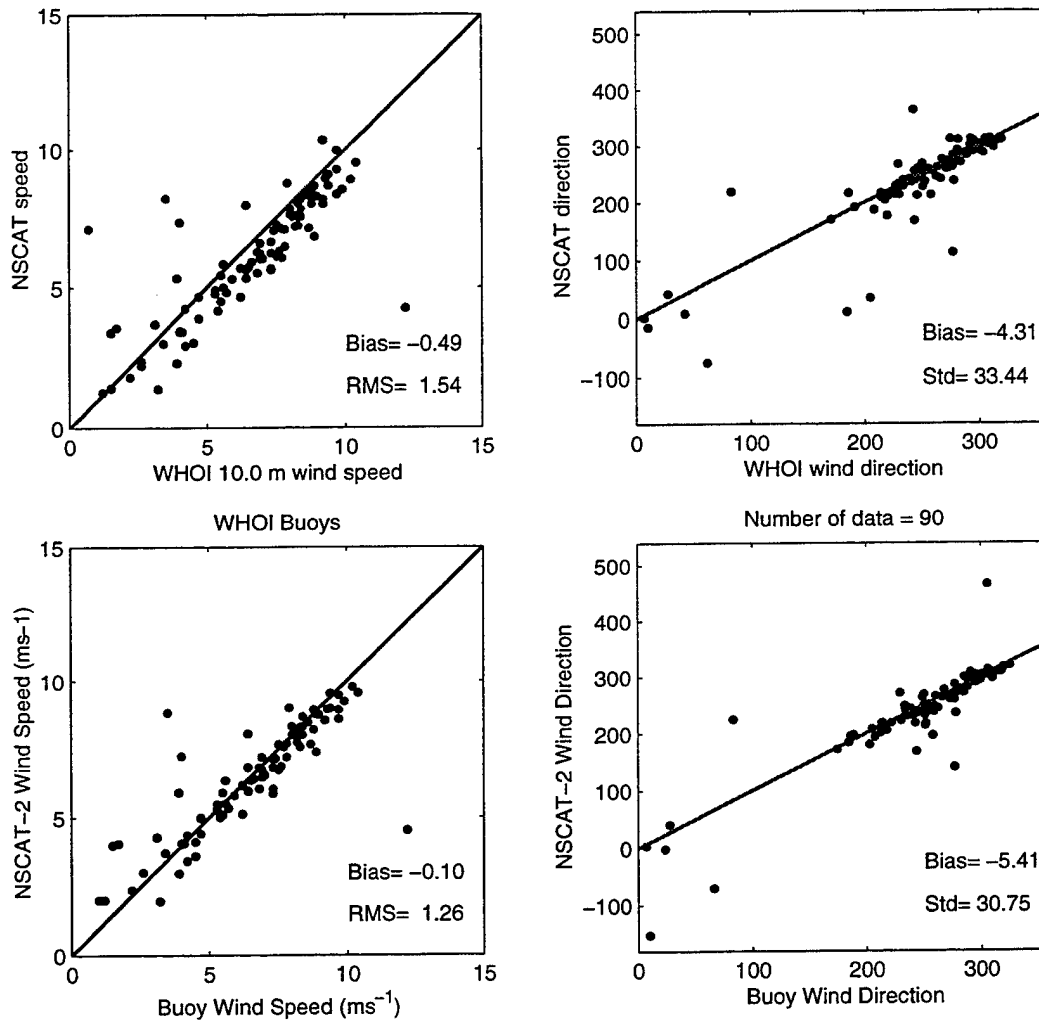


Figure 13: Scatterplots of wind speeds and directions derived from 25 km high resolution winds NSCAT-1 (top) and NSCAT-2 (bottom) with WHOI VAWR 10 m buoy winds. This comparison is similar to the TAO comparison where the NSCAT-2 wind speeds are closer to the buoy winds than the NSCAT-1 winds. The wind directions are similar for each of the model function, but are biased in the opposite direction to TAO directions.

#### 4.4.4 TAO/WHOI

To effectively compare the results of the WHOI buoys with the TAO array, the two TAO buoys closest to the WHOI buoys were selected to compare with NSCAT winds. TAO buoy 51307 (8°N, 125°W) is in closest proximity to the WHOI North buoy (10°N, 125°W) and TAO buoy 51017 (2°S, 125°W) is closest to WHOI South (3°S, 125°W).

In general, the TAO buoy wind speed statistics (Table 11) fall between the WHOI IMET and VAWR results. The wind direction biases are similar to the biases of the entire array at  $\sim 10^\circ$ . This shows that the bias differences between the entire TAO array and the WHOI buoys is not due to the buoy locations.

The scatterplots of buoys 51307 and 51017 (figure 14) highlight the similarities and differences a bit more clearly. The bias change between the two NSCAT model functions is evident and comparisons with WHOI IMET (figure 12) and VAWR (figure 13) shows that the distribution falls between the two WHOI sensors. The wind directions show that the NSCAT winds are clockwise with respect to the TAO buoy. Although there is a small counterclockwise bias for the VAWR and IMET winds, the majority of the co-locations appear unbiased.

Table 11: Comparison of NSCAT wind speeds and directions with TAO buoys 51017 and 51307 10 m winds. These buoys are the closest to the WHOI PACS buoys. See section 4.4.4 for a discussion of the results.

Product	Wind Speed Range $\text{ms}^{-1}$	Sample Size	Wind Speed				Wind Direction		Vector Correlation $\rho^2$
			Bias $\text{ms}^{-1}$	RMSE $\text{ms}^{-1}$	Correlation Coefficient	Symmetrical Regression	Bias (deg)	Std. D. (deg)	
NSCAT-1 25 km	0.0 – 50.0	107	-0.23	1.29	0.83	0.97	10.90	42.05	1.17
	0.0 – 5.0	29	0.22	1.65		1.16	18.59	74.64	0.26
	5.0 – 7.5	43	-0.34	1.24		0.96	8.04	29.25	1.07
	7.5 – 10.0	35	-0.47	0.96		0.95	11.50	21.94	1.55
NSCAT-1 50 km	0.0 – 50.0	86	-0.23	1.34	0.84	0.98	5.30	40.21	1.24
	0.0 – 5.0	24	-0.31	1.05		0.95	9.36	67.16	0.69
	5.0 – 7.5	36	-0.06	1.76		1.02	1.62	22.49	1.34
	7.5 – 10.0	26	-0.39	0.80		0.96	8.69	31.92	1.19
NSCAT-2 25 km	0.0 – 50.0	91	0.20	1.11	0.89	1.04	13.18	38.62	1.38
	0.0 – 5.0	25	0.21	1.00	0.96	1.10	26.30	62.15	0.45
	5.0 – 7.5	37	0.26	1.36	0.36	1.05	9.29	29.51	1.37
	7.5 – 10.0	29	0.10	0.83	0.94	1.02	11.25	22.59	1.60

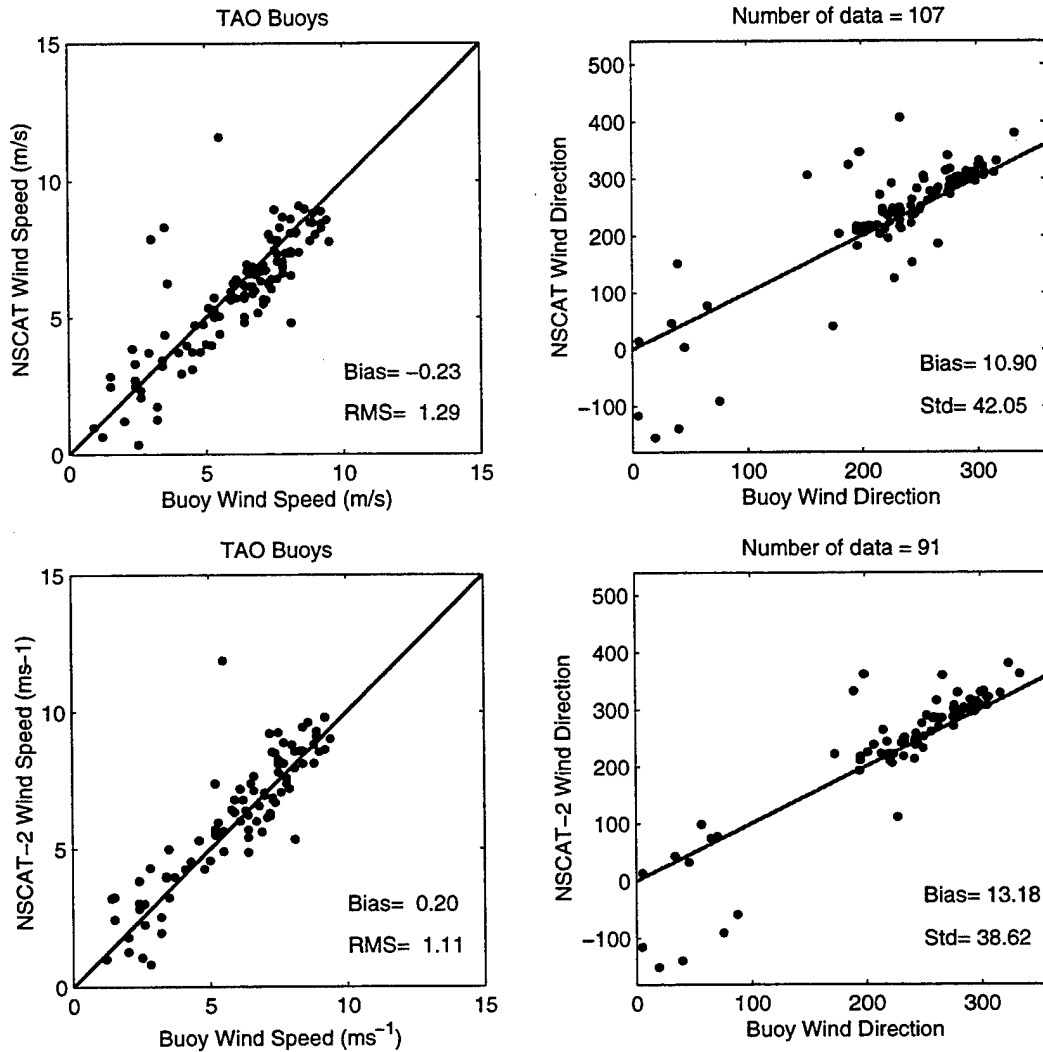


Figure 14: Scatterplots of wind speeds and directions derived from 25 km high resolution NSCAT-1 data (top) and NSCAT-2 (bottom) with TAO buoy #51017 and #51307 10 m buoy winds. These buoys are the closest to the WHOI PACS buoys. The TAO wind speed bias for these two buoys falls between the WHOI IMET and VAWR wind speeds. The wind direction bias is in the opposite direction to the WHOI winds and in the same direction as the entire TAO array.

### 4.5 Wind speed distributions

The distributions of wind speeds for the TAO co-locations, shown in figure 15 reflect the biases found in section 4.2. The wind speed bias is fairly uniform over the range of wind speeds measured in the equatorial Pacific. Although the number of co-locations is less, a similar offset exists for the VAWR co-locations (bottom panels of figure 16). The smaller positive bias for the IMET winds (top panels of figure 16) is not as apparent.

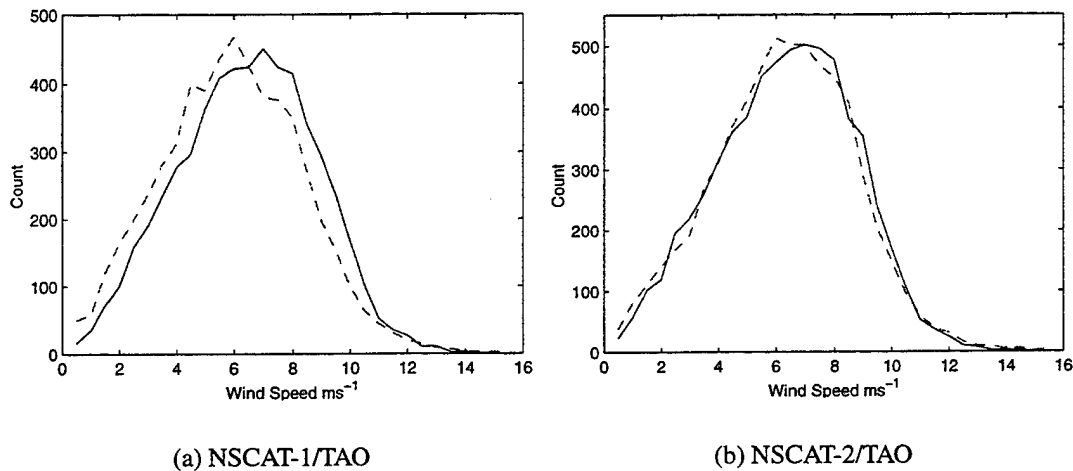


Figure 15: Wind speed distributions of TAO (solid) with NSCAT (dashed) (a) 25 km NSCAT-1 winds and (b) 25 km NSCAT-2 winds, binned in 0.5 ms<sup>-1</sup> wind speed bins. The overall bias in the NSCAT-1 winds is nearly eliminated in the NSCAT-2 winds. There remains a slight difference in the location of the peak distribution. The peak distribution of the NSCAT-2 winds is about 6 ms<sup>-1</sup>, while the peak of the TAO winds is about 7.5 ms<sup>-1</sup>.

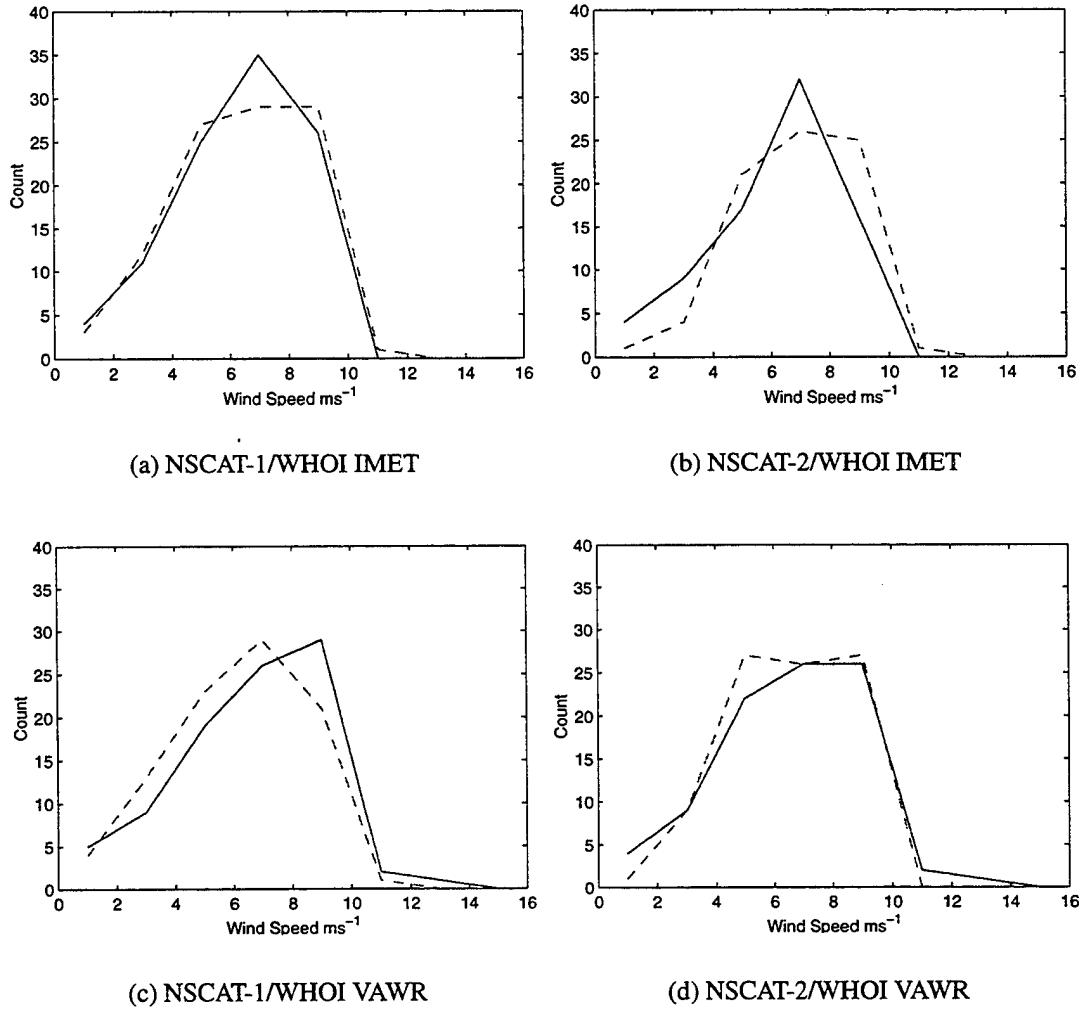


Figure 16: Wind speed distributions of WHOI (solid) and NSCAT (dashed) 10 m buoy winds; 25 km NSCAT-1 winds (left) and NSCAT-2 winds (right) compared to WHOI IMET 10 m buoy winds (upper) and WHOI VAWR 10 m buoy winds (lower). The winds distributions are binned in  $2.0 \text{ ms}^{-1}$  buoy wind speed bins. Although there are not as many co-locations as with the TAO array, the change in distribution of VAWR winds is similar to TAO. The NSCAT-2 distribution shows fewer low winds and more high winds than IMET.

### 4.6 Wind direction distributions

The winds in the tropical Pacific are predominately westward as shown by the direction distributions shown in figures 17–18. The most noticeable difference tends to be the broader distributions for the scatterometer. To a lesser extent, the distributions also show a higher number of scatterometer winds clockwise with respect to the buoys winds. The comparison of the NSCAT-1 and TAO directions also shows a difference in the north–south distributions. The TAO winds have more of a southward component while the NSCAT winds have more of a northward component to their westerly winds.

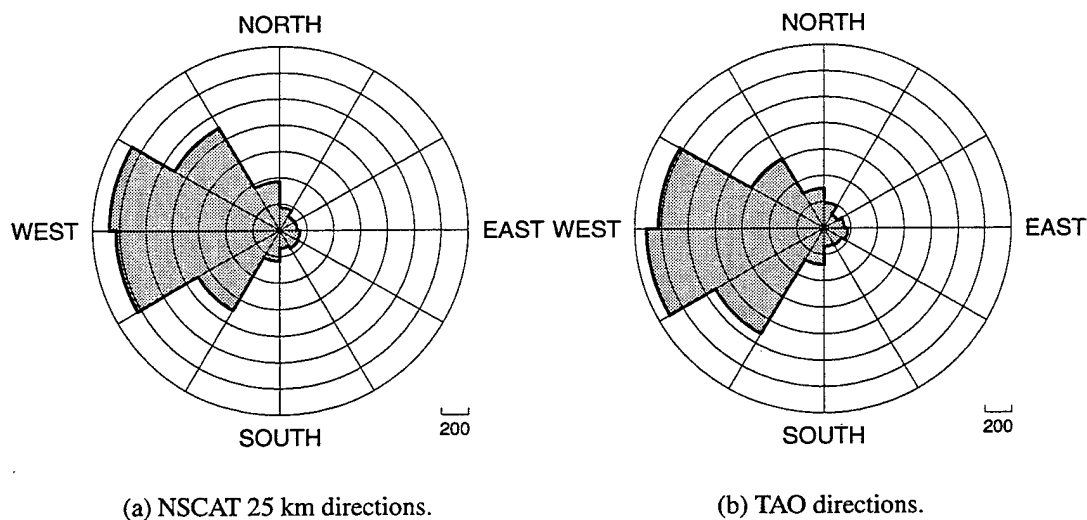


Figure 17: Wind direction distributions: (a) 25 km NSCAT-1 wind directions and (b) TAO 10 m buoy winds. The wind direction distributions are binned in 30° bins. The clockwise bias of the NSCAT winds with respect to the TAO winds can be seen.



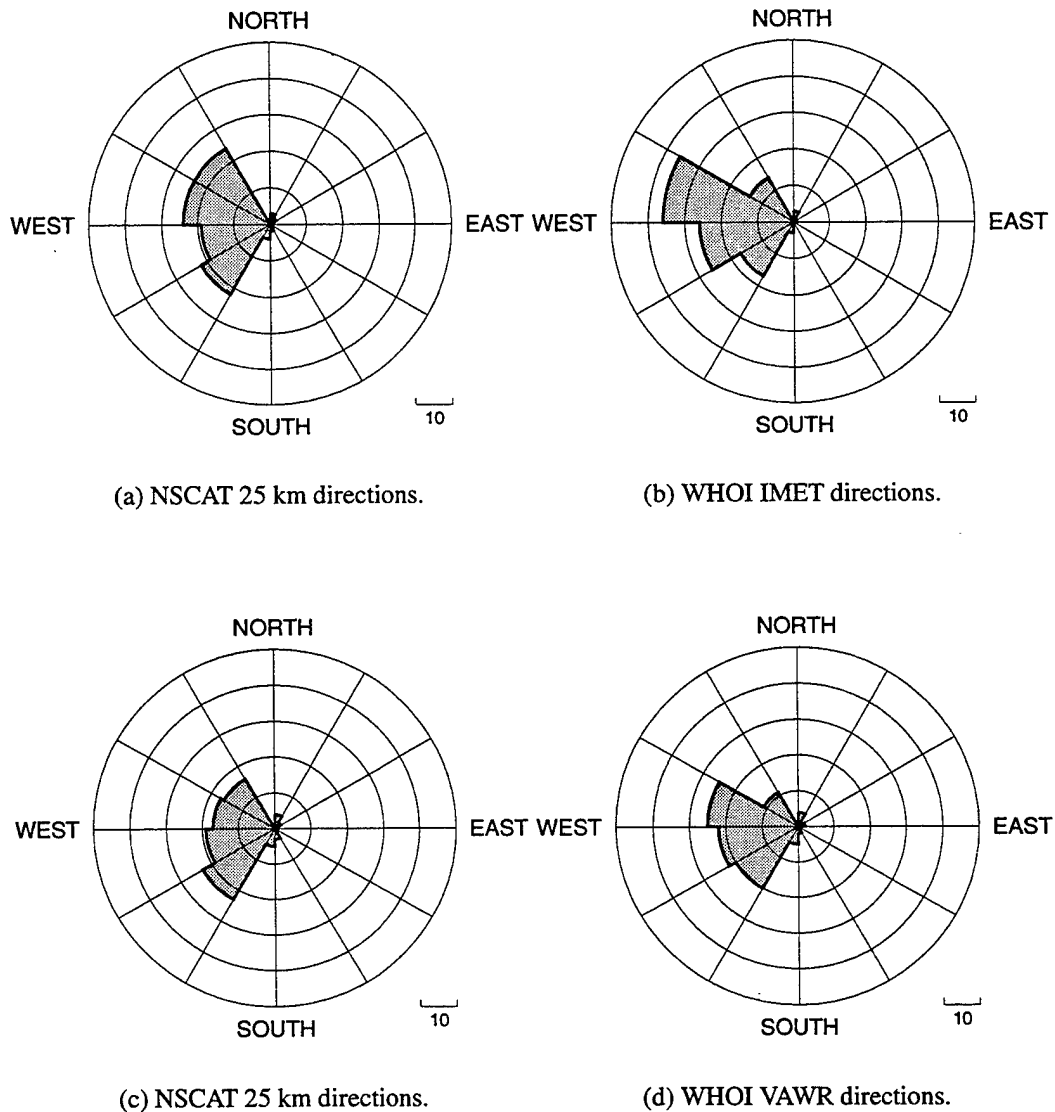


Figure 18: Wind direction distributions for 25 km NSCAT-1 (left) compared with: WHOI IMET buoy wind directions (top right) and VAWR (bottom right). The wind direction distributions are binned in 30° bins. Although the NSCAT wind directions had very little bias compared with IMET or VAWR winds, the distribution is broader than the WHOI IMET winds and more southward compared to the VAWR winds.

#### **4.7 Vector correlations**

The spatial distribution of the vector correlations (figure 19) shows a wide range of values with a low of 0.68 to a high of 1.76. Although a clear trend is not apparent, buoys near the center of the array ( $140^{\circ}\text{W} - 170^{\circ}\text{W}$ ), where the trade winds are most steady, tend to have higher coefficients.

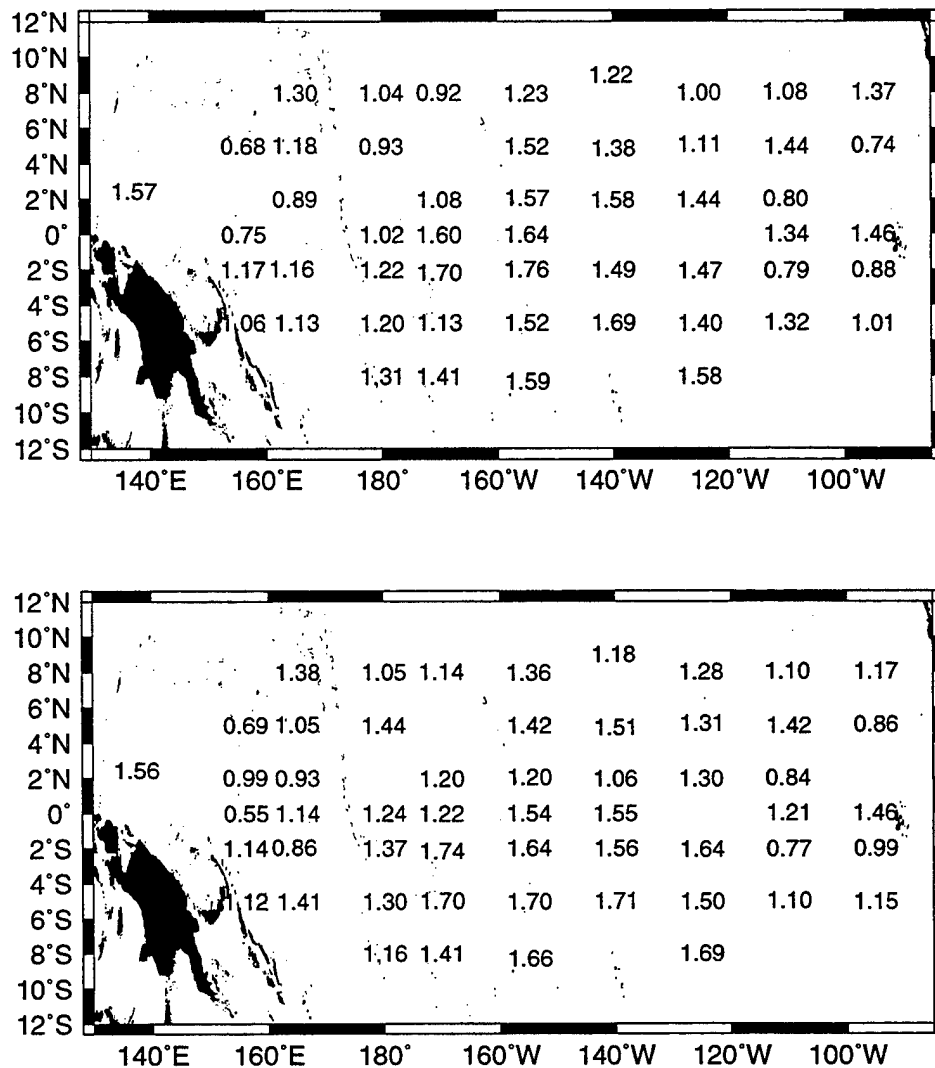


Figure 19: Spatial distribution for the vector correlation coefficient for each TAO buoy with NSCAT-1 (top) and NSCAT-2 (bottom) winds. Although the vector correlations do not present a clear spatial pattern, higher values tend to occur in the center of the array.

## 4.8 Directional Ambiguity

The empirical relationship between backscatter and wind retrieval produces up to four wind vectors. The NSCAT mid-beam antenna provides additional azimuthal measurements that should allow the determination of a unique wind vector. Tables 12 – 14 show the percentage of time each ambiguity was closest to the buoy wind direction. These tables show that the ambiguity removal technique is correctly selecting the closest vector  $\sim 90\%$  of the time. For the lower wind speeds ( $< 5.0 \text{ ms}^{-1}$ ), the closest vector is typically selected less often; about 75% for TAO and 80% for IMET and VAWR.

One problem still remains. Even with the third antenna there is an occasional  $180^\circ$  ambiguity, or flipped vector. Figure 20 shows the distribution of the percentage of flipped selected vectors with TAO buoy wind speed. Here, a vector is defined as flipped if it is more than  $120^\circ$  from the buoy wind direction. Although at moderate wind speeds ( $> 5.0 \text{ ms}^{-1}$ ) the percentage of flipped vectors is quite low at 1–2%, the lowest winds speeds have a much higher percentage of 10–20%. In the equatorial Pacific, these low winds represent a significant portion (20–25%) of the wind distribution, shown in figure 15.

We have not yet been able to statistically characterize these ambiguity errors, but there are several areas of interest. Figure 21 shows the percentage of flipped vectors as a function of buoy wind direction. This figure shows that the eastward winds exhibit a much higher percentage of the flipped vectors. These eastward winds (typically referred to as westerly wind bursts) are important to ocean models of the equatorial Pacific.

The median filter technique used may not remove patches of flipped vectors or shifts in the locations of fronts. Figure 22 shows a patch of eastward winds in a field of predominately westward winds at moderate speeds.

The wind retrievals with large direction errors do not significantly change the wind speed bias. By including all the co-located pairs of NSCAT/TAO wind data the overall wind speed bias is  $-0.54 \text{ ms}^{-1}$ , for the NSCAT-1 25km data set, as discussed in section 4.2. For comparison, if we consider only the co-located pairs with the direction differences within some specified limit, the speed bias changes. Figure 23 shows the scatterplots of 25 km winds from Figure 5, modified by limiting the angle differences to 90 and 60 degrees. The speed bias changes slightly from  $-0.54 \text{ ms}^{-1}$  to  $-0.58 \text{ ms}^{-1}$  and  $-0.61 \text{ ms}^{-1}$ , respectively.

Table 12: This table shows the percent of time each ambiguity was closest to the TAO buoy direction.

Product	Wind Speed	Sample Size	Ambiguity							
			1		2		3		4	
25 km NSCAT-1	0.0 – 50.0	5580	4851	(86.9%)	346	(6.2%)	274	(4.9%)	109	(2.0%)
	0.0 – 5.0	1523	1114	(73.1%)	197	(12.9%)	161	(10.6%)	51	(3.3%)
	5.0 – 7.5	2082	1869	(89.8%)	95	(4.6%)	80	(3.8%)	38	(1.8%)
	7.5 – 10.0	1634	155	(95.3%)	45	(2.8%)	22	(1.3%)	9	(0.6%)
	10.0 – 12.5	312	287	(92.0%)	8	(2.6%)	10	(3.2%)	7	(2.2%)
	12.5 – 50.0	29	23	(79.3%)	1	(3.4%)	1	(3.4%)	4	(13.8%)
50 km NSCAT-1	0.0 – 50.0	5196	4612	(88.8%)	331	(6.4%)	156	(3.0%)	97	(1.9%)
	0.0 – 5.0	1444	1123	(77.8%)	187	(13.0%)	78	(5.4%)	56	(3.9%)
	5.0 – 7.5	1887	1700	(90.1%)	98	(5.2%)	58	(3.1%)	31	(1.6%)
	7.5 – 10.0	1550	1491	(96.2%)	37	(2.4%)	15	(1.0%)	7	(0.5%)
	10.0 – 12.5	294	278	(94.6%)	9	(3.1%)	5	(1.7%)	2	(0.7%)
	12.5 – 50.0	21	20	(95.2%)	0	(0.0%)	0	(0.0%)	1	(4.8%)
25 km NSCAT-2	0.0 – 50.0	6334	5595	(88.3%)	338	(5.3%)	277	(4.4%)	124	(2.0%)
	0.0 – 5.0	1796	1330	(74.1%)	223	(12.4%)	177	(9.9%)	66	(3.7%)
	5.0 – 7.5	2353	2164	(92.0%)	74	(3.1%)	75	(3.2%)	40	(1.7%)
	7.5 – 10.0	1844	1783	(96.7%)	30	(1.6%)	21	(1.1%)	10	(0.5%)
	10.0 – 12.5	317	297	(93.7%)	9	(2.8%)	3	(0.9%)	8	(2.5%)
	12.5 – 50.0	24	21	(87.5%)	2	(8.3%)	1	(4.2%)	0	(0.0%)

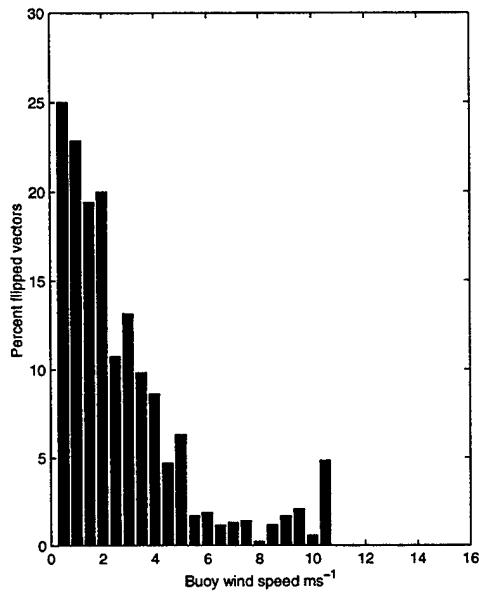
#### 4.8 Directional Ambiguity

Table 13: This table shows the percent of time each ambiguity was closest to the WHOI buoy IMET direction.

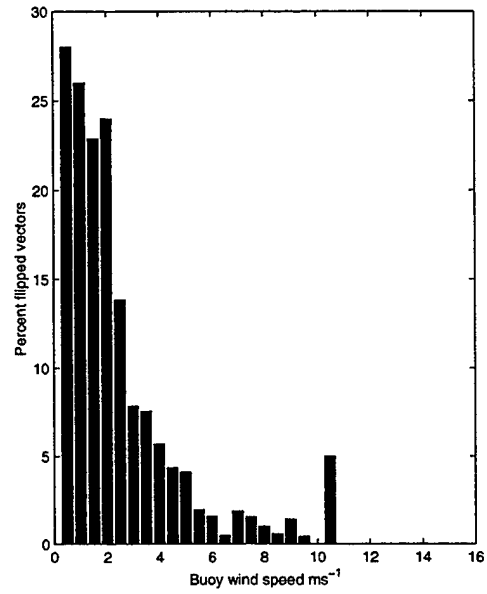
Product	Wind Speed	Sample Size	Ambiguity			
			1	2	3	4
25 km NSCAT-1	0.0 – 50.0	101	93 (92.1%)	6 (5.9%)	0 (0.0%)	2 (2.0%)
	0.0 – 5.0	25	21 (84.0%)	3 (12.0%)	0 (0.0%)	1 (4.0%)
	5.0 – 7.5	39	35 (89.7%)	3 (7.7%)	0 (0.0%)	1 (2.6%)
	7.5 – 10.0	37	37 (100.0%)	0 (0.0%)	0 (0.0%)	0 (0.0%)
50 km NSCAT-1	0.0 – 50.0	85	78 (91.8%)	5 (5.9%)	1 (1.2%)	1 (1.2%)
	0.0 – 5.0	18	14 (77.8%)	3 (16.7%)	0 (0.0%)	1 (5.6%)
	5.0 – 7.5	37	35 (94.6%)	1 (2.7%)	1 (2.7%)	0 (0.0%)
	7.5 – 10.0	30	29 (96.7%)	1 (3.3%)	0 (0.0%)	0 (0.0%)
25 km NSCAT-2	0.0 – 50.0	78	76 (97.4%)	0 (0.0%)	1 (1.3%)	1 (1.3%)
	0.0 – 5.0	20	18 (90.0%)	0 (0.0%)	1 (5.0%)	1 (5.0%)
	5.0 – 7.5	32	32 (100.0%)	0 (0.0%)	0 (0.0%)	0 (0.0%)
	7.5 – 10.0	26	26 (100.0%)	0 (0.0%)	0 (0.0%)	0 (0.0%)

Table 14: This table shows the percent of time each ambiguity was closest to the WHOI buoy VAWR direction.

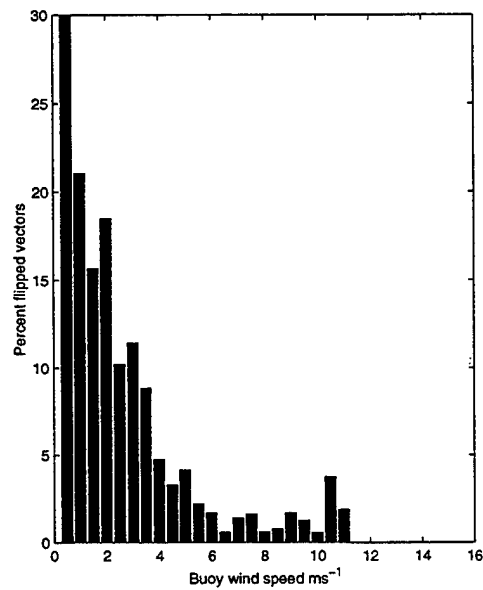
Product	Wind Speed	Sample Size	Ambiguity			
			1	2	3	4
25 km	0.0 – 50.0	91	84 (92.3%)	5 (5.5%)	0 (0.0%)	2 (2.2%)
	0.0 – 5.0	23	19 (82.6%)	3 (13.0%)	0 (0.0%)	1 (4.3%)
	5.0 – 7.5	28	25 (89.3%)	2 (7.1%)	0 (0.0%)	1 (3.6%)
	7.5 – 10.0	37	37 (100.0%)	0 (0.0%)	0 (0.0%)	0 (0.0%)
	10.0 – 12.5	3	3 (100.0%)	0 (0.0%)	0 (0.0%)	0 (0.0%)
50 km	0.0 – 50.0	92	81 (88.0%)	9 (9.8%)	1 (1.1%)	1 (1.1%)
	0.0 – 5.0	25	19 (76.0%)	5 (20.0%)	0 (0.0%)	1 (4.0%)
	5.0 – 7.5	29	26 (89.7%)	2 (6.9%)	1 (3.4%)	0 (0.0%)
	7.5 – 10.0	36	34 (94.4%)	2 (5.6%)	0 (0.0%)	0 (0.0%)
	10.0 – 12.5	2	2 (100.0%)	0 (0.0%)	0 (0.0%)	0 (0.0%)
25 km	0.0 – 50.0	90	85 (94.4%)	3 (3.3%)	2 (2.2%)	0 (0.0%)
	0.0 – 5.0	24	20 (83.3%)	2 (8.3%)	2 (8.3%)	0 (0.0%)
	5.0 – 7.5	30	29 (96.7%)	1 (3.3%)	0 (0.0%)	0 (0.0%)
	10.0 – 12.5	3	3 (100.0%)	0 (0.0%)	0 (0.0%)	0 (0.0%)



(a) NSCAT-1 25 km winds.



(b) NSCAT-1 50 km winds.



(c) NSCAT-2 25 km winds.

Figure 20: Percentage flipped vectors as a function of TAO buoy wind speed.

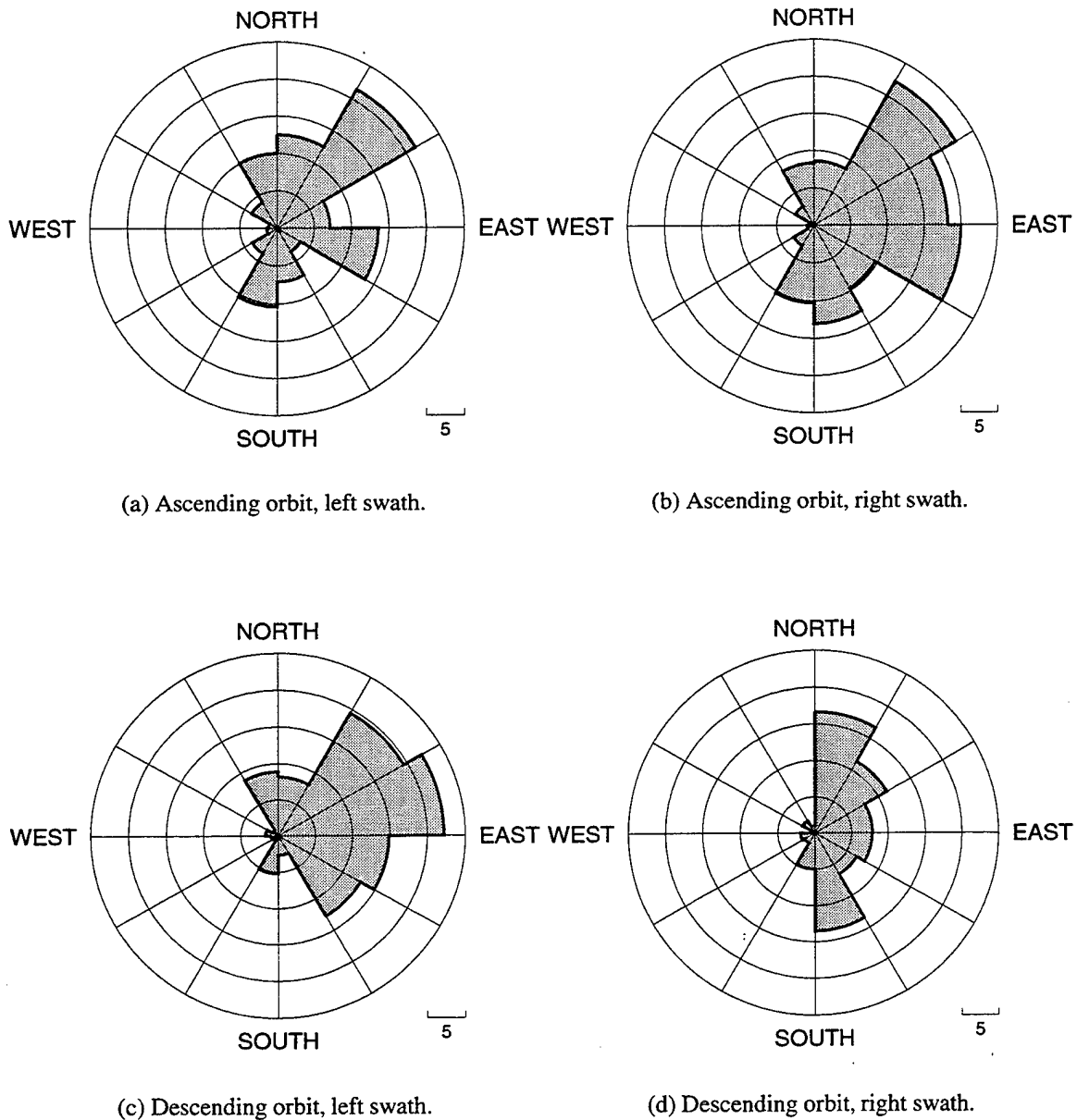


Figure 21: Percentage of flipped vectors from NSCAT-1 25 km winds as a function of buoy wind direction for various orbital geometries. The flipped vectors are binned in 30° bins and the circles represent 5% errors.



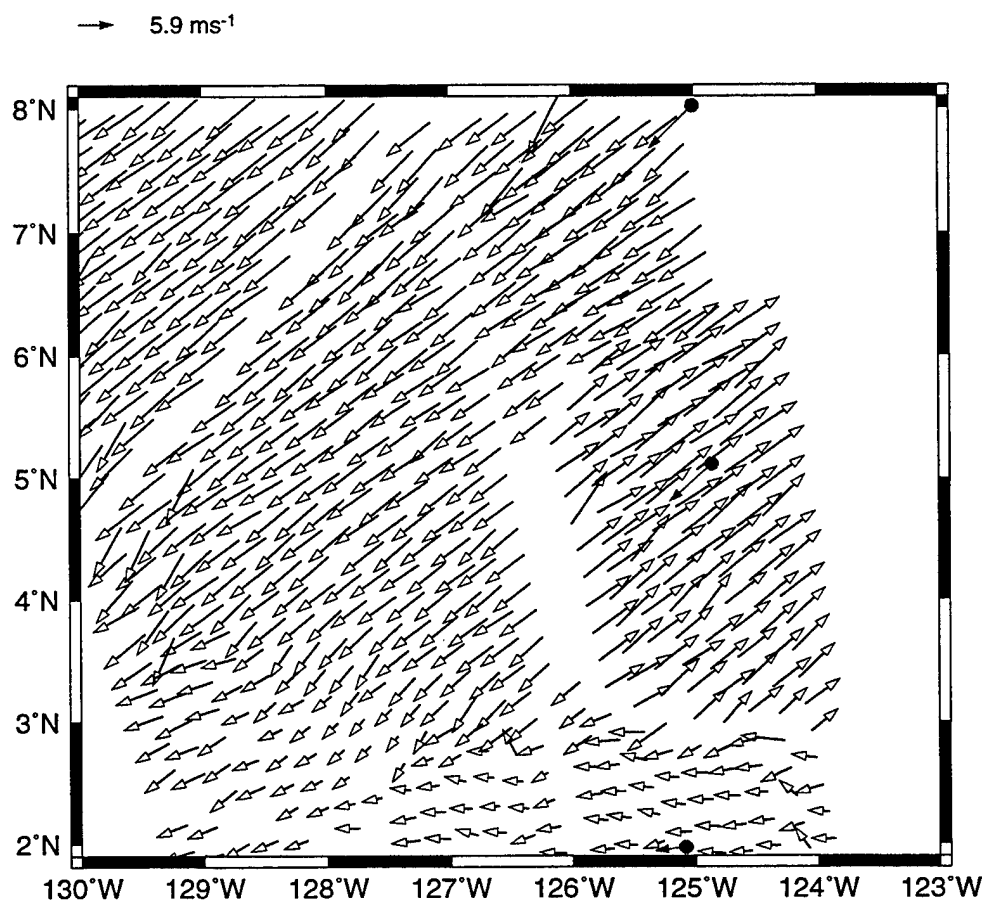


Figure 22: NSCAT wind vectors (open vectors) compared with TAO wind vectors (closed vectors with circles) on February 26, 1997.

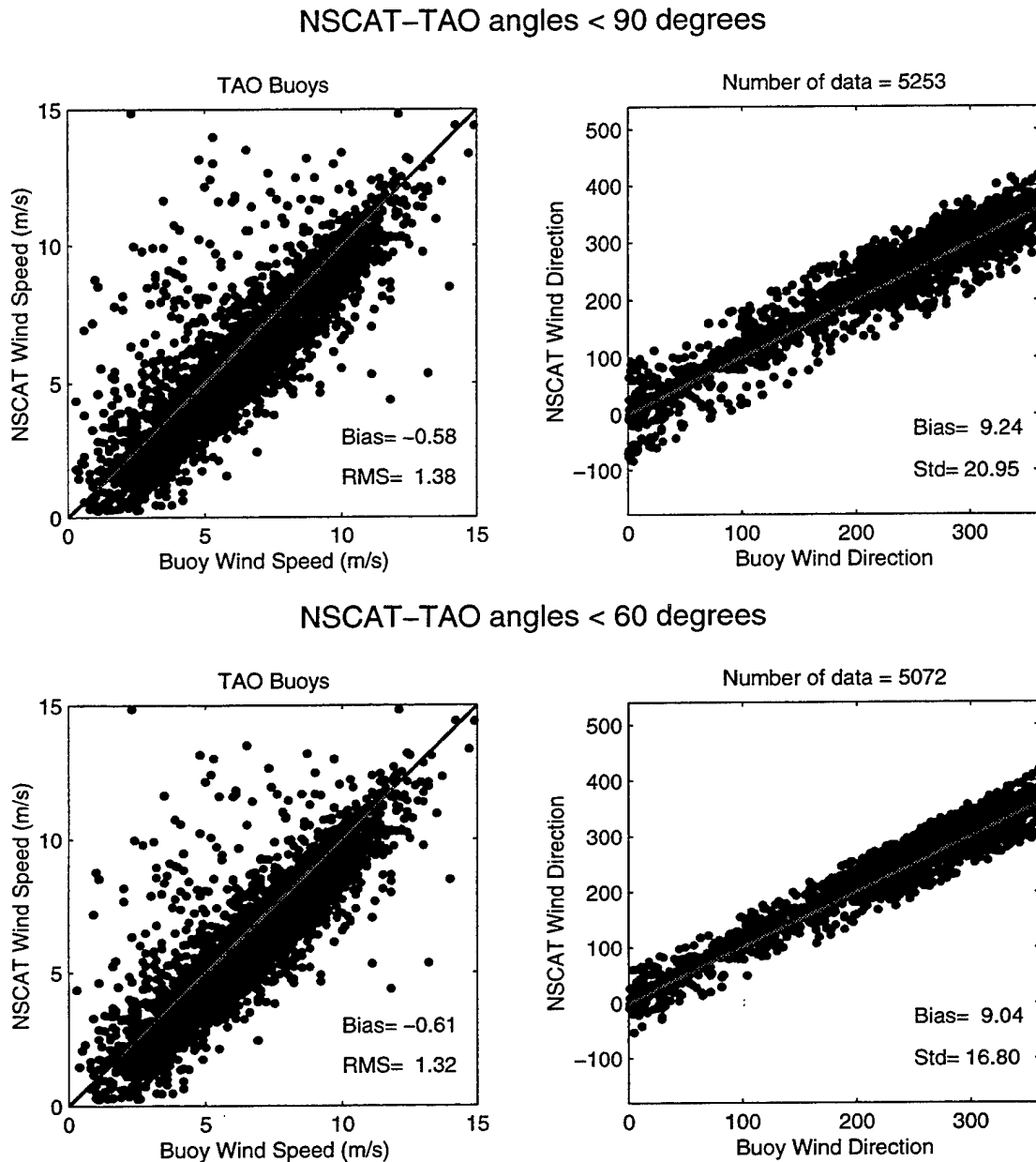


Figure 23: Scatterplots of wind speeds (left) and directions (right) comparing TAO winds with NSCAT 25 km high resolution data for angles differing by 90° or less (top) and by 60° or less (bottom). Overall bias and RMS values in lower right of each panel. There were 5253 co-locations within 90° and 5072 co-locations within 60°.

#### 4.9 Surface currents

Several TAO buoys along the equator contained mechanical current meters and acoustic doppler current profilers (ADCPs). The upper mechanical current meter (10 m depth) was compared with wind speed bias (figure 24). This figure shows that when the surface current is aligned with the wind, the buoy wind report is higher than the scatterometer. When the current is opposing the wind, the scatterometer wind speed is higher. These differences are in the expected sense, since the scatterometer measures winds relative to the ocean surface, which is moving.

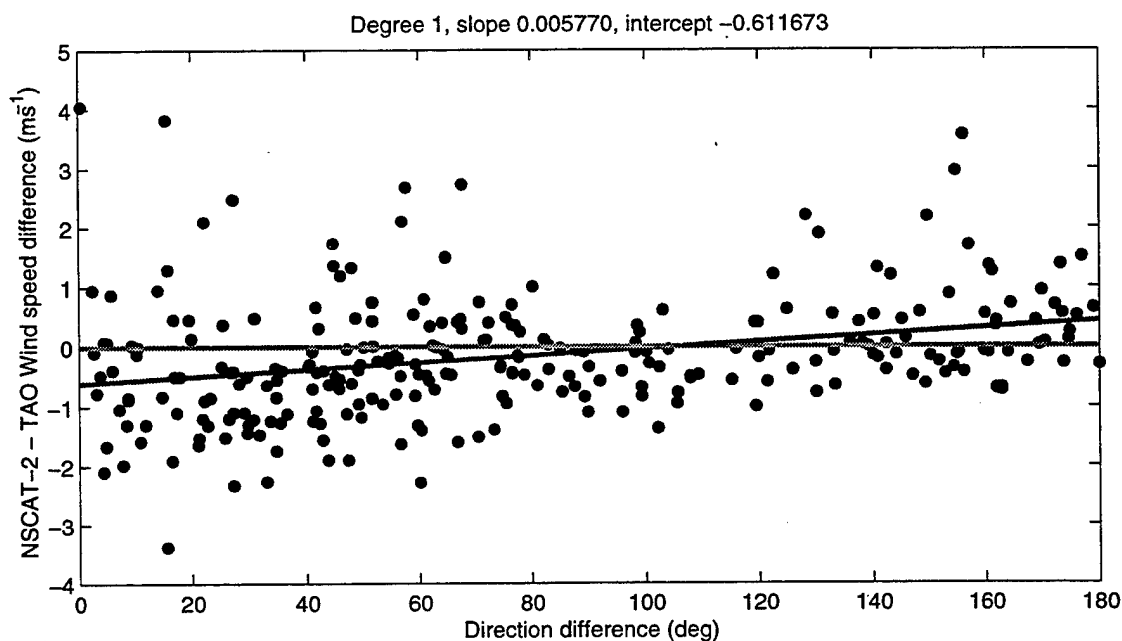


Figure 24: The wind speed difference scatterometer - buoy ( $S - B$ ) dependence on the angle between wind and surface (10 m depth) currents measured from TAO buoys at the equator.

#### 4.10 Rain

Rain striking the sea surface will effect the scatterometer power levels (Bliven and Giovannangeli, 1993). The rain gauges on several of the TAO buoys were analyzed to determine the effects of rain on the returned wind. Unfortunately, only seven co-locations contained any rain information and were not used.

---

## 5 Summary

More than 5000 co-located pairs of TAO and NSCAT data collected over the ten months of the NSCAT mission from September 1996 to June 1997 were compared. The data were taken within about  $8^\circ$  of the equator, spanning the Pacific Ocean. Two WHOI buoys, which collected data along  $125^\circ\text{W}$  over that last three months of the NSCAT mission, added another 300 co-located pairs to our analysis. All buoy data were normalized to 10 m height in a neutrally stratified atmosphere. Three sets of NSCAT data were analyzed; the standard winds with 50 km cells and the high resolution winds with 25 km cells using the NSCAT-1 model function; and high resolution winds reprocessed with the NSCAT-2 model function. The NSCAT data were required to be within 30 minutes and one WVC of the buoy data. Most of the buoy wind speeds fell between 3 and  $10\text{ ms}^{-1}$  and the predominant directions were westward, as expected in the equatorial Pacific Ocean. The similarity of statistics for the co-located data from the 25 km and the 50 km wind products validated the high quality of the 25 km winds. The NSCAT-2 model function significantly improved the wind speed comparison, but did not affect the wind direction bias.

The wind speed bias of NSCAT-1 scatterometer wind retrievals is about  $0.5\text{ ms}^{-1}$  lower than the winds measured by the TAO buoy array, with an RMSE of about  $1.5\text{ ms}^{-1}$ . The WHOI VAWR wind measurements confirm this negative bias, although the scatterometer winds compare quite well to the WHOI IMET wind data, with a very small positive wind speed bias. The scatterometer winds compare best with the TAO winds at mid-speeds, in the northern and western regions in the TAO buoy array domain, towards the outer cells of the swaths and in moderately unstable (near  $-2^\circ$ ) atmospheric surface layers. The scatterometer underestimates the buoy winds at wind speeds greater than  $10\text{ ms}^{-1}$ . The largest wind speed differences are typically due to the scatterometer overestimating the wind speed. There was insufficient information to attribute this to rain.

The wind speed bias of NSCAT-2 scatterometer wind retrievals is less than  $0.1\text{ ms}^{-1}$  for TAO and WHOI VAWR winds while the bias with the WHOI IMET winds increased to  $0.6\text{ ms}^{-1}$ . There was improvement in most of the wind speed statistics when the NSCAT-2 model function was used. NSCAT-2 produced a significantly better symmetrical regression over the entire wind speed range.

The wind direction biases of the NSCAT-1 and NSCAT-2 scatterometer wind retrievals are less than about  $10^\circ$ , but they are positive, resulting in scatterometer winds that are on average clockwise from the TAO winds. The overall standard deviation of wind direction is rather high at over  $30^\circ$ , but by neglecting the high variability of the low winds the RMSE is closer to  $20^\circ$ . Comparisons with VAWR direction data show a smaller negative bias, whereas the IMET aligns best with the scatterometer wind data. The directional scatter is highest at wind speeds less than  $3\text{ ms}^{-1}$ .

Even with a third antenna on the NSCAT scatterometer, the four wind vector solutions could not always be reduced to the correct one, resulting in large direction differences between the scatterometer and the buoy winds, around 4% of the time. We defined flipped NSCAT vectors as those that were  $120^\circ$  or more away from the buoy wind directions. Most of these flipped vectors occurred with eastward buoy winds. The negative wind speed bias changed slightly when the flipped vectors were omitted from the co-location data set, suggesting that the wrong vector solution not only has the wrong direction but the wrong speed as well. The average vector correlation coefficient for the NSCAT/TAO co-located time series is 1.4. When the co-located pairs with a flipped vector were removed from the time series, the vector correlation coefficient increased to 1.6. Geographically, the vector correlation coefficients were higher in the south and central region of the TAO buoy array domain.

## Acknowledgments

This work is supported by NASA under contract number 957652.

Thanks are due to Linda Stratton who performed much of the data quality control at PMEL, and to Paul Freitag for the rainfall and PROTEUS mooring data. Data access was facilitated by Linda Mangum, Dai McClurg, and Margie McCarty. The analysis and visualization tool Ferret, developed by Steve Hankin at PMEL, was invaluable in database maintenance, graphics production, and quality control. We would also like to thank Steve Anderson and Robert Weller and the WHOI Upper Ocean Processes Group for the quick access to PACS buoy data. Finally, the NSCAT team at JPL has been extremely helpful and efficient processing and reprocessing the data.

---

## 6 References

- Beardsley, R.C., E.P. Dever, S.J. Lentz and J.P. Dean, 1998. Surface heat flux variability over the northern California shelf. *J. Geophys. Res.*, **Vol 103**, C10, 21553-21586.
- Bliven, L. and J-P. Giovanangeli, 1993a. An experimental study of microwave scattering from rain- and wind-roughened seas, *International Journal of Remote Sensing*, **14(5)**, 855-869.
- Crosby, D.S., L.C. Breaker and W.H. Gemmill, 1993. A Proposed Definition for Vector Correlation in Geophysics: Theory and Application. *J. Atmos. Oceanic Tech.*, **10**, 355-367
- Dunbar, R. S. NASA Scatterometer High-Resolution Merged Geophysical Data Product User's Guide Version 1.1. JPL, March 1997
- Freilich, M.H. and R.S. Dunbar, 1999. The accuracy of the NSCAT 1 vector winds: Comparisons with National Data Buoy Center buoys. *J. Geophys. Res.* **104**, 11,231-11,246.
- Freilich, M.H., H. Qi, and R.S. Dunbar, A Ku-band scatterometer model function from NSCAT measurements and operational global surface wind analyses (in production) 1999.
- Freilich, M.H., 1997. Validation of Vector Magnitude Datasets: Effects of Random Component Errors. *J. Atmos. Oceanic Tech.*, **Vol 14**, 3, 695-703.
- Graber, H.C., N. Ebuchi and R. Vakkayil, 1996. Evaluation of ERS-1 scatterometer winds with wind and wave ocean buoy observations, *RSMAS Tech. Rept.*, RSMAS 96-003.
- Hosom, D, R. Weller, R. Payne and K. Prada, 1995. The IMET (Improved METeorology) Ship and Buoy Systems. *J. Atmos. Oceanic Tech.*, **Vol 12**, 3, 527-540.
- Liu, W.T. and W. Tang, 1996. Equivalent Neutral Wind, Jet Propulsion Laboratory, JPL 96-17.
- Liu, W.T., K.B. Katsaros and J.A. Businger, 1979. Bulk Parameterization of Air-sea Exchanges of Heat and Water Vapor Including the Molecular Constraints at the Interface, *J. Atmos. Oceanic Tech.*, **36**, 1722-1735.
- Mangum, L.J., H.P. Freitag and M.J. McPhaden, 1994: TOGA-TAO array sampling schemes and sensor evaluations. *Proc. OCEANS '94 OSATES*, **Vol II**, 13-16.

- McPhaden, M., 1995. The Tropical Atmosphere Ocean (TAO) Array is completed. *Bull. Amer. Meteor. Soc.*, **Vol 76**, 5.
- Jet Propulsion Laboratory (JPL), 1998. NASA Scatterometer Science Data Product User's Manual; Overview & Geophysical Data Products Version 1.2. JPL D-12985, Pasadena, CA
- Rufenach, C., 1998. Comparison of Four ERS-1 Scatterometer Wind Retrieval Algorithms with Buoy Measurements, *J. Atmos. Oceanic Tech.*, **Vol 15** 304–313.
- Weller, R.A., D.L. Rudnick, R.E. Payne, J.P. Dean, N.J. Pennington and R.P. Trask, 1990. Measuring Near-Surface Meteorology over the Ocean from an Array of Surface Moorings in the Subtropical Convergence Zone, *J. Atmos. Oceanic Tech.*, **Vol 7** 85–103.
- Wentz, F.J. and D.K. Smith, 1999. A model function for the ocean normalized radar cross section at 14 GHz derived from NSCAT observations. *J. Geophys. Res.*, **104**, 11,499–11,514
- Wentz, F.J., S. Peteherych, and L.A. Thomas, 1984: A model function for ocean radar cross sections at 14.6 GHz. *J. Geophys. Res.*, **89**, 3689–3704.
- Yamartino, A., 1984. A comparison of several “single-pass” estimators of the standard deviation of wind direction. *J. Climate Appl. Meteor.*, **23**, 1362–1366.

## DOCUMENT LIBRARY

*Distribution List for Technical Report Exchange – July 1998*

University of California, San Diego  
SIO Library 0175C  
9500 Gilman Drive  
La Jolla, CA 92093-0175

Hancock Library of Biology & Oceanography  
Alan Hancock Laboratory  
University of Southern California  
University Park  
Los Angeles, CA 90089-0371

Gifts & Exchanges  
Library  
Bedford Institute of Oceanography  
P.O. Box 1006  
Dartmouth, NS, B2Y 4A2, CANADA

NOAA/EDIS Miami Library Center  
4301 Rickenbacker Causeway  
Miami, FL 33149

Research Library  
U.S. Army Corps of Engineers  
Waterways Experiment Station  
3909 Halls Ferry Road  
Vicksburg, MS 39180-6199

Marine Resources Information Center  
Building E38-320  
MIT  
Cambridge, MA 02139

Library  
Lamont-Doherty Geological Observatory  
Columbia University  
Palisades, NY 10964

Library  
Serials Department  
Oregon State University  
Corvallis, OR 97331

Pell Marine Science Library  
University of Rhode Island  
Narragansett Bay Campus  
Narragansett, RI 02882

Working Collection  
Texas A&M University  
Dept. of Oceanography  
College Station, TX 77843

Fisheries-Oceanography Library  
151 Oceanography Teaching Bldg.  
University of Washington  
Seattle, WA 98195

Library  
R.S.M.A.S.  
University of Miami  
4600 Rickenbacker Causeway  
Miami, FL 33149

Maury Oceanographic Library  
Naval Oceanographic Office  
Building 1003 South  
1002 Balch Blvd.  
Stennis Space Center, MS, 39522-5001

Library  
Institute of Ocean Sciences  
P.O. Box 6000  
Sidney, B.C. V8L 4B2  
CANADA

National Oceanographic Library  
Southampton Oceanography Centre  
European Way  
Southampton SO14 3ZH  
UK

The Librarian  
CSIRO Marine Laboratories  
G.P.O. Box 1538  
Hobart, Tasmania  
AUSTRALIA 7001

Library  
Proudman Oceanographic Laboratory  
Bidston Observatory  
Birkenhead  
Merseyside L43 7 RA  
UNITED KINGDOM

IFREMER  
Centre de Brest  
Service Documentation - Publications  
BP 70 29280 PLOUZANE  
FRANCE



<b>REPORT DOCUMENTATION PAGE</b>	<b>1. REPORT NO.</b> <b>WHOI-99-10</b>	<b>2.</b>	<b>3. Recipient's Accession No.</b>
<b>4. Title and Subtitle</b> Evaluation of NSCAT Scatterometer Winds Using Equatorial Pacific Buoy Observations			<b>5. Report Date</b> July 1999
			<b>6.</b>
<b>7. Author(s)</b> Michael J. Caruso, Suzanne Dickinson, Kathryn A. Kelly, Mick Spillane Linda J. Mangum, Michael J. McPhaden, Linda D. Stratton			<b>8. Performing Organization Rept. No.</b> WHOI-99-10
<b>9. Performing Organization Name and Address</b>  Woods Hole Oceanographic Institution Woods Hole, Massachusetts 02543			<b>10. Project/Task/Work Unit No.</b>
			<b>11. Contract(C) or Grant(G) No.</b> (C) 957652 (G)
<b>12. Sponsoring Organization Name and Address</b>  NASA			<b>13. Type of Report &amp; Period Covered</b> Technical Report
			<b>14.</b>
<b>15. Supplementary Notes</b> This report should be cited as: Woods Hole Oceanog. Inst. Tech. Rept., WHOI-99-10.			
<b>16. Abstract (Limit: 200 words)</b> As part of the calibration/validation effort for NASA's Scatterometer (NSCAT) we compare the satellite data to winds measured at the sea surface with an array of buoys moored in the equatorial Pacific Ocean. The NSCAT data record runs from September, 1996 through the end of June, 1997. The raw NSCAT data, radar backscatter, is converted to wind vectors at 10 meters above the surface assuming a neutrally stratified atmosphere, using the NSCAT-1 and NSCAT-2 model functions. The surface winds were measured directly by the TAO (Tropical Atmosphere Ocean) buoy array which spans the width of the equatorial Pacific within about 8° of the equator. The buoy program and data archive are maintained by the Pacific Marine Environmental Laboratory, at the National Oceanic and Atmospheric Administration, in collaboration with institutions in Japan, France and Taiwan. We also use data from two buoys maintained by the Woods Hole Oceanographic Institution located along 125°W. Since the buoy winds are measured at various heights above the surface, they are adjusted for both height and atmospheric surface layer stratification before comparisons are made to the NSCAT data. Co-location requirements include measurements within 100 km and 60 minutes of each other. There was a total of 5580 comparisons for the NSCAT-1 model function and 6364 comparisons for the NSCAT-2 model function. The NSCAT wind speeds, using the NSCAT-1 model function, are lower than the buoy wind speeds by about 0.54 ms <sup>-1</sup> and have a 9.8° directional bias. The NSCAT-2 winds speeds were lower than the TAO buoy winds only 0.08 ms <sup>-1</sup> , but still have the same 9.8° directional bias. The wind retrieval algorithm selects the vector closest to the buoy approximately 88% of the time. However, in the relatively low wind speed regime of the TAO array, approximately 4% of the wind vectors are more than 120° from the buoy wind.			
<b>17. Document Analysis</b>			
<b>a. Descriptors</b> scatterometer buoy calibration validation			
<b>b. Identifiers/Open-Ended Terms</b>			
<b>c. COSATI Field/Group</b>			
<b>18. Availability Statement</b>  Approved for public release; distribution unlimited.	<b>19. Security Class (This Report)</b> <b>UNCLASSIFIED</b>	<b>21. No. of Pages</b> 64	
	<b>20. Security Class (This Page)</b>	<b>22. Price</b>	